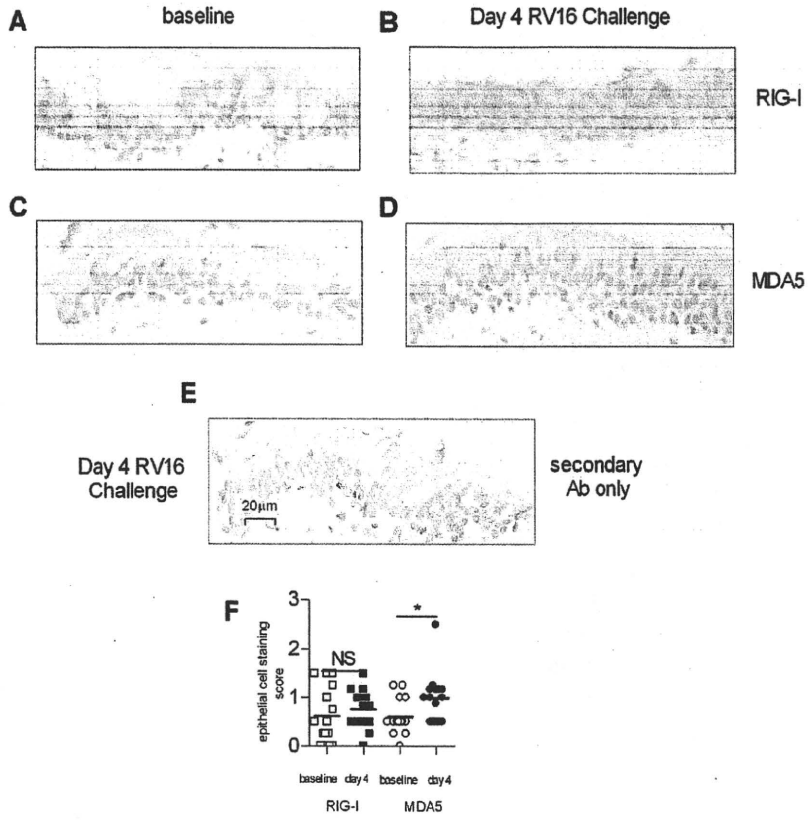

Figure 2. RIG-I and MDA5 expression in bronchial biopsy tissue following *in vivo* RV16 infection. Normal individuals underwent fibre-optic bronchoscopy at baseline or day 4 following RV16 challenge, and bronchial biopsies were taken, and assessed for RIG-I protein by immunohistochemistry at baseline (A) and day 4 post RV16 challenge (B). Biopsies were also assessed for MDA5 protein at baseline (C) and day 4 post RV16 challenge (D). Positive staining is indicated by the brown coloration, localized to the columnar epithelial cells. Background staining was assessed by incubating a Day 4 biopsy with secondary antibody only (E). Staining scores of bronchial epithelium showing increases at day 4 compared to baseline (F) *$p<0.05$ as indicated, NS = not significant. Scale is indicated by the horizontal bar.
doi:10.1371/journal.ppat.1001178.g002

TLR3, RIG-I and MDA5 are required for maximal RV induced pro-inflammatory cytokine gene expression

The role of TLR3, RIG-I and MDA5 on the T cell chemokines rantes and IP-10, and the neutrophil chemokines IL-8 and ENA-78 were also investigated. Figure 5 shows that TLR3, RIG-I and MDA5 siRNA all reduced RV1B induced rantes compared to control siRNA (Figure 5A,E,I). Likewise, TLR3, RIG-I and MDA5 siRNA all reduced RV induced IP-10 (Figure 5B,F,J). TLR3, RIG-1 and MDA5 siRNA also reduced RV induced IL-8 mRNA (Figure 5C,G,K). Finally TLR3, RIG-I and MDA5 siRNA also reduced RV1B induced ENA-78 compared to control siRNA (Figure 5D,H,L). In support of the above, siRNA specific for Cardif and TRIF reduced all RV1B induced pro-inflammatory cytokines compared to control siRNA (Figure S2).

Inhibition of RIG-I and MDA5 increased RV replication

As RIG-I and MDA5 were required for RV1B induced IFN-β and both IFN-β and IFN-λ gene expression respectively, we next reasoned that their role was not redundant and that abrogation of either RNA helicase would result in increased RV replication in HBECs. Figure 6A demonstrates that after 24 h post infection, RV16 RNA levels were increased after transfection with siRNA specific for RIG-I compared to control siRNA. RV1B RNA levels were also increased. Also, using siRNA specific for MDA5, an increase in RV1B RNA was observed, compared to cells transfected with control siRNA, and RV16 RNA levels were slightly increased compared to control siRNA. In the same experiments, virus release was also determined by titration assay, 48 h after infection. Figure 6B demonstrates that transfection with RIG-I specific siRNA resulted in increased RV16 release compared to control siRNA and slightly increased RV1B virus release. Conversely, transfection with MDA5 specific siRNA resulted in higher RV1B release, and a small increase in RV16 virus release compared to control siRNA. Furthermore, transfection of the bronchial epithelial cell line BEAS-2B, with dominant negative RIG-I (RIG-IC), resulted in enhanced replication of RV16 RNA (Figure 6C), at 24 h and RV16 virus release at 48 h post infection (Figure 6D). Transfection of constitutively active RIG-I (ΔRIG-I) resulted in up to 60 fold suppression of RV1B and 47 fold suppression of RV16 virus release at 48 h (Figure S3). This data further implicates the RNA helicase RIG-I in RV recognition and induction of anti-viral activity.

RV induced RIG-I and MDA5 gene expression involved TLR3/TRIF signalling

As RV1B infection induced both early RIG-I and early MDA5 protein and mRNA production, and both are required

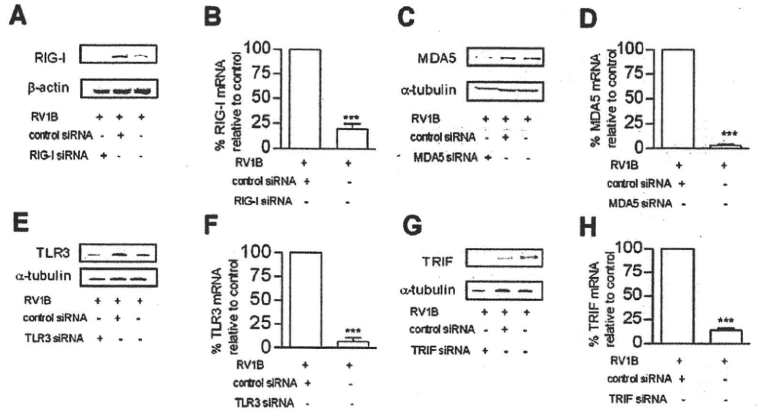

Figure 3. Effects of each siRNA on RIG-I, MDA5, TLR3 and TRIF mRNA and protein levels. HBECs were transfected with siRNA specific for RIG-I or control siRNA, infected with RV1B and RIG-I protein (A) and mRNA (B) measured. HBECs were transfected with MDA5 specific siRNA or control siRNA and infected with RV1B and MDA5 protein (C) and mRNA (D) measured. HBECs were transfected with siRNA specific for TLR3 or control siRNA and infected with RV1B and TLR3 protein (E) and mRNA (F) measured. HBECs were transfected with siRNA specific for TRIF or control siRNA and infected with RV1B and TRIF protein (G) and mRNA (H) measured. *$p<0.05$, **$p<0.01$, ***$p<0.001$ versus control siRNA or as indicated. mRNA data was generated from 6 independent experiments utilizing 3 independent HBEC donors, 2 experiments per donor.
doi:10.1371/journal.ppat.1001178.g003

for maximal anti-rhinoviral activity, we sought to identify the receptor(s) responsible for RNA helicase induction. As RV enters via the endosome, we hypothesized that TLR3 was responsible for increased RIG-I and MDA5 gene expression. In order to investigate the relationship between TLR3/TRIF signaling and RIG-I and MDA5 gene expression in RV

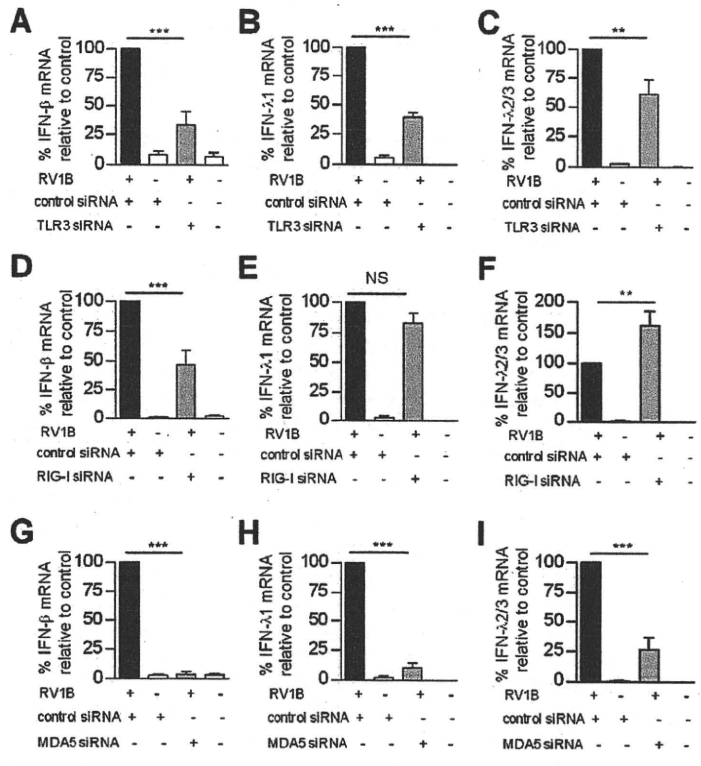

Figure 4. Role of TLR3, RIG-I and MDA5 in RV1B induced IFN-β, and IFN-λ gene expression in HBECs. HBECs were transfected with control siRNA or siRNA specific for TLR3 (A–C), RIG-I (D–F), MDA5 (G–I), and infected with RV1B. IFN-β (A,D,G), IFN-λ1 (B,E,H) and IFN-λ2/3 (C,F,I) mRNA were measured 24 h post infection **$p<0.01$, ***$p<0.001$ versus control siRNA, NS = not significant. mRNA data was generated from 6 independent experiments utilizing 3 independent HBEC donors, 2 experiments per donor.
doi:10.1371/journal.ppat.1001178.g004

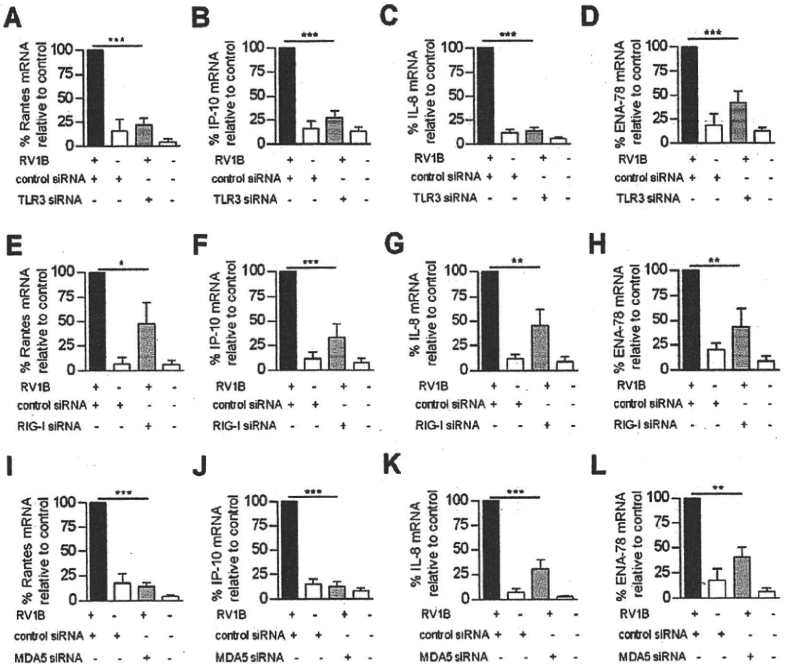

Figure 5. Role of TLR3, RIG-I and MDA5 in RV1B induced pro-inflammatory cytokine gene expression in HBECs. HBECs were transfected with control siRNA or siRNA specific for TLR3 (A–D), RIG-I (E–H), MDA5 (I–L), and infected with RV1B. Rantes (A,E,I), IP-10 (B,F,J), IL-8 (C,G,K), and ENA-78 (D,H,L) mRNA were measured 24 h post infection *$p<0.05$, **$p<0.01$, ***$p<0.001$ versus control siRNA. *$p<0.05$, **$p<0.01$, ***$p<0.001$ versus control siRNA or as indicated. mRNA data was generated from 6 independent experiments utilizing 3 independent HBEC donors, 2 experiments per donor.

doi:10.1371/journal.ppat.1001178.g005

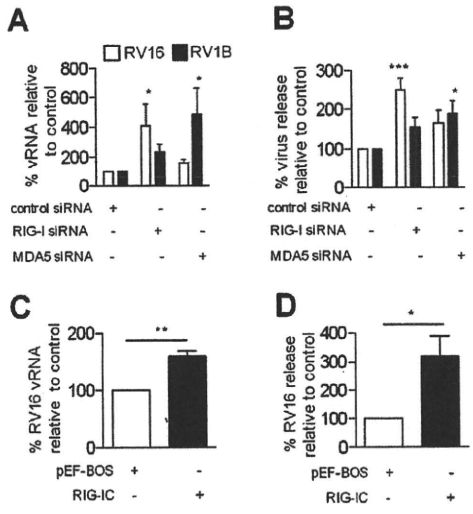

Figure 6. Effects of RIG-I and MDA5 abrogation on RV replication in HBECs. HBECs were transfected with siRNA specific for RIG-I, MDA5 or control siRNA, infected with RV1B or RV16 and vRNA determined by PCR at 24 h (A) or RV release by titration at 48 h (B). BEAS-2B cells were transfected with 0.5 μg RIG-IC or pEF-BOS control, and RV16 vRNA (C) and virus release (D) determined. mRNA data was generated from 5 independent experiments utilizing 3 independent HBEC donors, 2 experiments per donors 1,2 and a one experiment for donor 3; and 4 independent experiments for BEAS-2B cells.

doi:10.1371/journal.ppat.1001178.g006

infection, we next assessed if specific knockdown of TLR3 and the adaptor TRIF affected RV1B induced RNA helicase gene expression. Figure 7 demonstrates that siRNA specific for TLR3 reduced RV1B induced RIG-I mRNA versus control siRNA, (Figure 7A), and reduced RV1B induced MDA5 mRNA (Figure 7B). Consistent with the sequential affect of TLR3 on RNA helicase induction, we found that RIG-I specific siRNA did not affect TLR3 mRNA levels compared to control siRNA (Figure 7C), and MDA5 specific siRNA also did not affect TLR3 mRNA levels compared to control siRNA (Figure 7D). Furthermore, siRNA specific for the TLR3 adaptor TRIF, reduced RV1B induced RIG-I mRNA (Figure 7E) and also RV1B induced MDA5 mRNA compared to control siRNA (Figure 7F). In each experiment, knockdown of TRIF mRNA by TRIF specific siRNA was confirmed, and we also confirmed knockdown of TRIF protein at 48 h post transfection (Figure 3G,H). Using a plasmid encoding constitutively active TRIF (ΔTRIF), the reverse of the above results were obtained in HBECs (Figure 7G,H). Transfection with ΔTRIF significantly increased both RIG-I and MDA5 gene expression, compared to empty vector control (pUNO1). Furthermore, incubation of HBECs with the TLR3 ligand polyIC induced RIG-I mRNA from 4–24 h post treatment (Figure 7I) and MDA5 from 8–24 h (Figure 7J). PolyIC treatment also induced RIG-I and MDA5 protein by 4–12 h post treatment as shown by western blotting (Figure 7K) and immunofluorescence (Figure 8A). Finally siRNA specific for TLR3 or TRIF reduced polyIC induced RIG-I and MDA5 protein (Figure 8B), strongly implicating TLR3/TRIF mediated signal transduction in RV induced RNA helicase induction in HBECs.

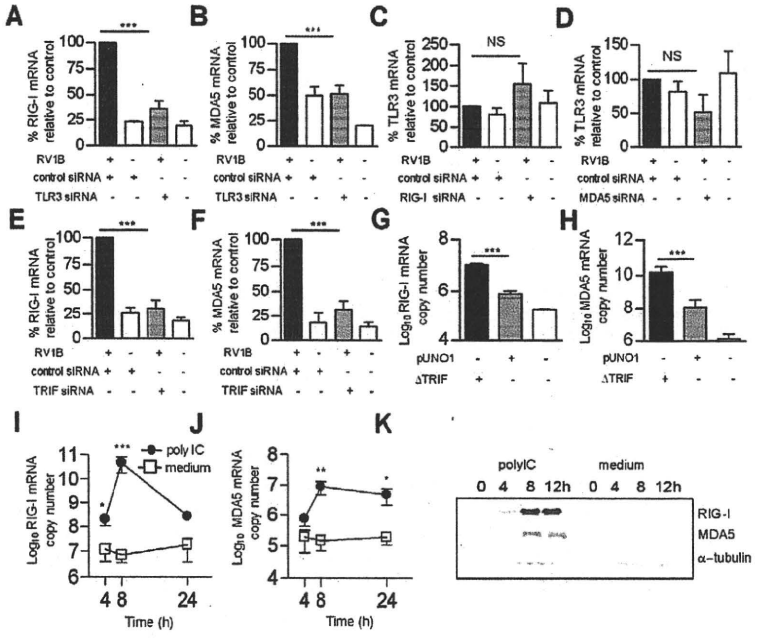

Figure 7. Role of TLR3 and TRIF in RV1B induced RIG-I and MDA5 expression. HBECs were transfected with siRNA specific for TLR3 or control siRNA (A,B) RIG-I or control siRNA (C) or MDA5 or control siRNA (D), TRIF or control siRNA (E,F) infected with RV1B, and RIG-1 (A,E), MDA5 (B,F) or TLR3 mRNA (C,D) measured at 24 h. HBECs were transfected with ΔTRIF or pUNO1 plasmids, or were left untransfected, and RIG-I (G) and MDA5 mRNA (H) measured 24 h post transfection. HBECs were treated with the TLR3 ligand polyIC or medium and RIG-I (I) and MDA5 mRNA (J) measured at various time points, or RIG-I and MDA5 protein assessed by western blotting over time (K). *$p<0.05$, **$p<0.01$, ***$p<0.001$ versus control siRNA, pUNO1, or medium treated cells, NS = not significant. mRNA data was generated from 5 independent experiments utilizing 3 independent HBEC donors, 2 experiments per donors 1,2 one experiment for donor 3.
doi:10.1371/journal.ppat.1001178.g007

RV1B infection *in vivo* resulted in initial increased RIG-I and MDA5 expression in the absence of type I and type III IFN signalling

As RV induced RIG-I and MDA5 occurred early, and in a TLR3/TRIF dependent manner, and as the TLR3 and TRIF pathway leads to IRF3 activation and IFN-β and IFN-λ induction, we assessed the role of IFN signalling in RV1B induced RIG-I and MDA5. In our *in vitro* experiments with HBECs, it was difficult to rule out the role of endogenous, or RV induced early IFN-β/λ inducing RIG-I and MDA5. We therefore ultilised *IFNAR1* deficient mice, in a mouse model of RV1B infection [39]. *IFNAR1* deficient mice are devoid of IFN-α/β signaling, and spleen cells have recently been shown to have reduced IFN-λ (IL-28B) production *in vitro* and lack IFN-λ within the vagina *in vivo* [40]. Figure 9 shows that following RV1B infection, *IFNAR1* deficient mice produced a low level of IFN-β within the lung but did not produce IFN-λ, however wildtype controls produce both IFN-β mRNA at 24 h (Figure 9A) and IFN-λ mRNA at 48 h (Figure 9B). At 8 h post infection, RV1B infection of *IFNAR1* deficient mice and wildtype mice both resulted in increased RIG-I (Figure 9C) and MDA5 gene expression compared to time 0 h, (Figure 9D). The induction of RIG-I and MDA5 was biphasic for both *IFNAR1* deficient and wildtype mice, wildtype mice produced higher levels of RIG-I and MDA5 mRNA at 16 h post infection, and at 48 h post infection for RIG-I only. Cytoplasmic protein from lung homogenates were extracted and probed for RIG-I and MDA5 protein by western blotting. Both *IFNAR1*$^{-/-}$ and wildtype mice exhibited increased RIG-I and MDA5 protein at 8 h compared to mock infected controls. At later time points (24 h and 48 h) wildtype mice had more RIG-I and MDA5 protein compared to *IFNAR1* deficient mice, likely caused by IFN signaling (blots are shown in Figure 9E and densitometry compared to α-tubulin shown in Figure 9F&G). This data therefore shows that initial RV induced RIG-I and MDA5 is IFN independent, and that at later time points, further virus replication increases in RIG-I and MDA5 gene expression later on in *IFNAR1*$^{-/-}$ mice, and in wildtypes further virus replication and IFN signaling events contribute to later lung RNA helicase mRNA expression.

Discussion

Viral dsRNA and ssRNA are recognised by at least two independent pattern recognition pathways, composed of TLR3, and TLR7/8 in the endosome and the RNA helicases RIG-I, MDA5 in the cytoplasm. Previous studies have employed well established models of virus infection, however similar studies using viruses important to human disease in their natural host cell type *in vivo* are largely yet to be performed. In the present study, we describe the role of TLR3 and RNA helicases in the recognition of RV infection in primary HBECs, the main cell type infected in the lower respiratory tract *in vivo*. RV is an important human pathogen, responsible for a range of illnesses including asthma exacerbations. We have used both major group RV16 and minor group RV1B (approximately 77% genome identity) in our studies, as both these groups represent the majority of RVs involved in human disease. Understanding the basis of RV recognition and signalling leading to IFN and pro-inflammatory cytokines could potentially lead to new therapeutic targets for RV associated illnesses.

We found that TLR3, RIG-I and MDA5 were required for IFN-β while MDA5 and TLR3 were required for maximal IFN-

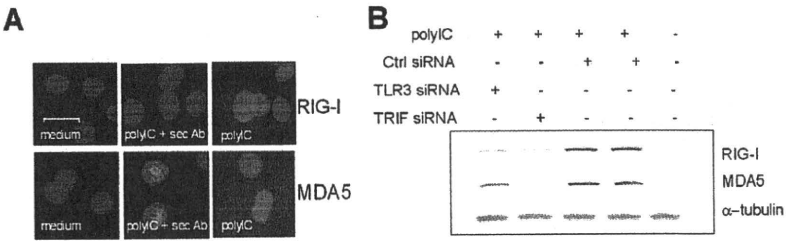

Figure 8. Role of TLR3 and TRIF in polyIC induced RIG-I and MDA5 protein. HBECs were treated with polyIC or medium and examined using immunofluorescence at 24 h for RIG-I *(upper panel,* A*)* and MDA5 *(lower panel,* A*)*. Both cytoplasmic RIG-I and MDA5 (in green) was induced after polyIC treatment at 24 h, compared to medium treated cells, or cells stained with secondary antibody only. Horizontal line indicates 20 μm scale. HBECs were treated with polyIC or medium for 8 h and the effects of TLR3 and TRIF siRNA on polyIC induced RIG-I and MDA5 assessed by western blotting (B). TLR3 and TRIF siRNA reduced RIG-I and MDA5 protein compared to control siRNA. α-tubulin was used to control for protein loading.
doi:10.1371/journal.ppat.1001178.g008

λ1 and IFN-λ2/3 mRNA expression. We then hypothesized that the most likely explanation for the dual requirement of both endosomal and cytoplasmic recognition systems and the importance of both RIG-I and MDA5 for IFN-β expression was that the endosomal and cytoplasmic recognition pathways were in some way linked, and their sequential activation was required for maximal IFN-β and IFN-λ gene expression. This is in contrast to other studies, which have observed mostly cell type specific differences concerning RIG-I/MDA5 and the TLR family members, with murine embryonic fibroblasts (MEFs) and conventional dendtitic cells (DCs) utilizing RIG-I and MDA5 for virus induced IFN production [25,36] while plasmacytoid DCs use TLRs including TLR3 [35,36]. Despite these findings, a recent study has reported the induction of type I IFN after i.p. injection of polyIC, to be reduced in $TRIF^{-/-}$ and $IPS\text{-}1^{-/-}$ double deficient mice, compared to either $IPS^{-/-}$ or $TRIF^{-/-}$ mice [41]. A number of recent *in vitro* studies have also reported a role for both TLR and RNA helicase signalling in polyIC induced responses, [42–45]. In short, explanations for differences between these results are likely due to cell type dependence on one pattern recognition system versus another, and the models of virus infection employed. We argue that for structural cells, including epithelial cells at mucosal surfaces, these cells may have evolved a dual dependency on both endosomal and intracellular recognition systems, which may be dissimilar for leukocytes including DCs. Hence as a first line defense against viral infection, efficient IFN production is an outcome of both TLR and RNA helicase mediated signalling working together.

The siRNA experiments we performed have demonstrated the requirement of TLR3 and MDA5 for IFN-λs, but TLR3, RIG-I and MDA5 for IFN-β gene expression. TLR3, RIG-I and MDA5 were also all important for a range of pro-inflammatory cytokines, including T cell chemokines rantes and IP-10 and neutrophil chemokines IL-8 and ENA-78. These results confirm and expand on recent data by Wang et al [46], using BEAS-2B cells and specific siRNA transfection, Wang et al showed that MDA5, TRIF but not RIG-I was important for RV induced IFN-β, IFN-λs and several interferon stimulated genes (ISGs). The role of MDA5 was confirmed in primary tracheobronchial epithelial cells. However why or how MDA5 and TLR3 are both required for RV infection in these studies was not analyzed in any depth. Our observation of RIG-I being important for IFN-β in HBECs could be due differences between BEAS-2B cells and HBECs, or differences in efficiency of siRNA knockdown of target mRNA. Our data also show that the RIG-IC DN also increases RV replication in BEAS-2B cells, again suggests a role for RIG-I in RV responses. Why RIG-I was not required for IFN-λ expression in our studies is unclear. Possible explanations for these results could be that MDA5 siRNA was more consistent at reducing the target mRNA compared to RIG-I siRNA, or that at the time point studied (24 h), MDA5 is more important than RIG-I in IFN-λ expression. IFN-β and the IFN-λs are both IRF3 responsive [47], and it is possible that for RV infection, MDA5 is more efficiently activated, resulting in robust signalling and IRF3 activation. Recently, it has been shown that IRF3 activation is complex, requiring multiple kinases for maximal phosphorylation and activation [48]. It is possible that differences exist between RIG-I and MDA5 signaling to IRF3, or IFN-β and IFN-λ promoters have different requirements for IRF3 activation. It has also previously been observed that siRNA transfection can interfere with endogenous RNA sensing molecules [49,50] and induce spontaneous IFN or cytokine production. All our siRNA were used to minimize potential off-target effects; they were used as pools of four individual siRNAs, and were designed with minimal known stimulatory sequences and also contained 3′ UU overhangs to minimize activation of RIG-I, which can be activated by siRNA [49]. We were careful to assess the likelihood of spontaneous induction of IFN or cytokines studied by all siRNA, and we did not observe significant induction for control or any specific siRNA. Therefore, we are confident that our results using siRNA are accurately describing the role of each molecule in RV dependent responses, and are not confounded due to siRNA recognition by endogenous processes or are the result of obvious off-target effects.

Initial experiments into the specificity of RIG-I suggested it bound *in vitro* transcribed and/or 5′-triphosphorylated ssRNA [33–35], and therefore could not recognize the RNA of picornaviruses such as encephalomyocarditis virus (EMCV) which do not synthesize 5′-triphosphosphorylated ssRNA. This has been questioned recently with the observation that RIG-I can bind low weight dsRNA [32]. Other than EMCV, little is known about the role of RIG-I in the infection of Picornaviruses. Our data provide definitive evidence that both RIG-I and MDA5 are important in innate responses to RV infection. Knockdown of both RIG-I and MDA5 produced higher viral loads of major group RV16 and minor group RV1B, again providing evidence that RIG-I can recognize the RNA of Picornaviruses. As the 7kB RV genome replicates in a RNA dependent manner, we argue that dsRNA molecules are present during replication in the cytoplasm. Hence, it is plausible that dsRNA of differing sizes could potentially ligate both RNA helicases. Future studies to confirm these interactions, such as immunoprecipitation studies are necessary to investigate the exact nature of the RNA species that RIG-I and MDA5 are binding to in the context of RV infection in HBECs.

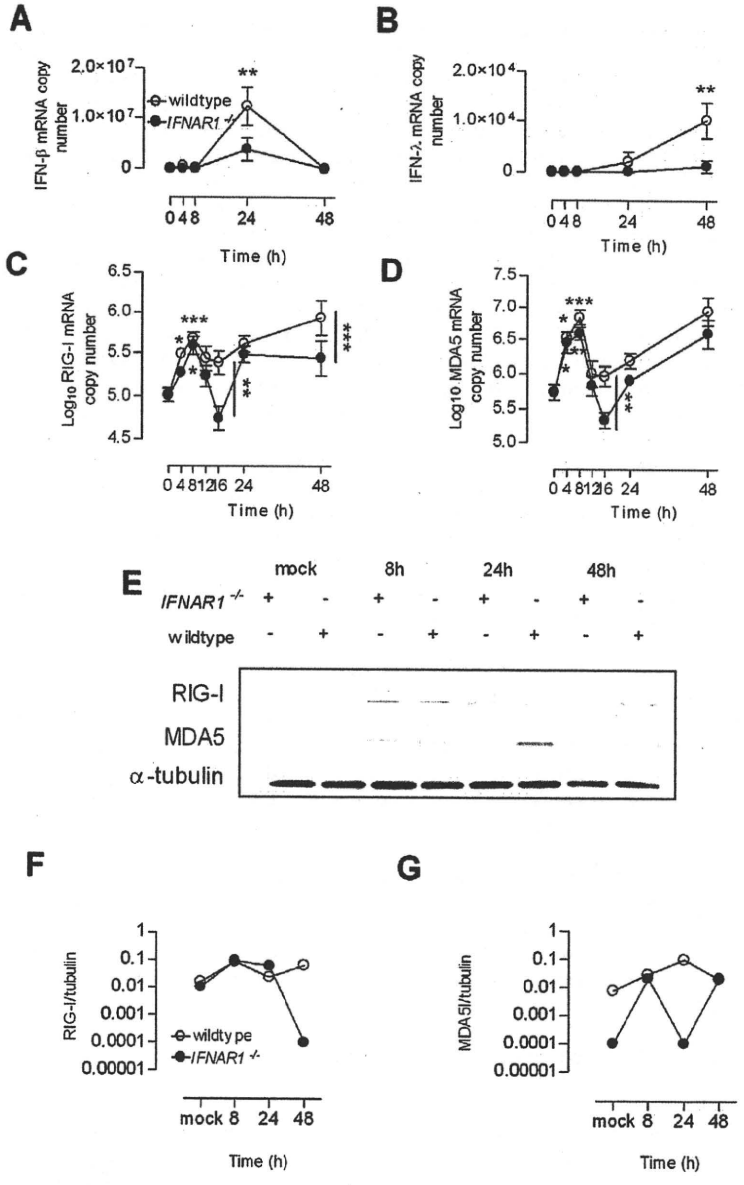

Figure 9. Expression of RIG-I and MDA5 mRNA and protein in wildtype and *IFNAR1* deficient mice. Wildtype 129/SvJ and *IFNAR1*$^{-/-}$ mice were infected with RV1B and lung protein and mRNA analysed over time. In wildtype mice, and to a lesser extent, *IFNAR1*$^{-/-}$ mice, RV1B induced IFN-β mRNA (A), and IFN-λ mRNA only in wildtype mice (B), and induced RIG-I in both wildtype and *IFNAR1*$^{-/-}$ mice (C). RV1B also induced MDA5 in both wildtype and *IFNAR1*$^{-/-}$ mice (D). In both wildtype and *IFNAR1*$^{-/-}$ mice, RIG-I and MDA5 mRNA induction was evident by 8 h post infection. RV1B also induced RIG-I and MDA5 protein by 8 h in both wildtype and *IFNAR1*$^{-/-}$ mice, measured by western blot (E), and RIG-I and MDA5 protein as a ratio of α-tubulin protein measured by densitometry over time is also shown (F&G respectively) *$p<0.05$, **$p<0.01$ ***$p<0.001$ versus time 0 h or as indicated.

doi:10.1371/journal.ppat.1001178.g009

Having established that TLR3, RIG-I and MDA5 were all required for innate responses and that RIG-I and MDA5 protein was not constitutively expressed in HBECs, whereas TLR3 was constitutively expressed, we hypothesized that RIG-I and MDA5 could be induced by TLR3 activation. While we did not study the early events of viral entry, RV has been used as a model Picornavirus and their biology has been extensively studied. RV enters via the endosome where the acidified environment is essential to viral uncoating and release of +ve sense ssRNA. [51,52]. Despite being a ssRNA virus, the 7kB ssRNA genome contains some secondary structures [53,54], including the 5′ multiple stem loop structure, containing the ribosome entry site, which has been previously visualized in endosomes during virus uncoating [55]. As RV infection requires the formation of mature endosomes, and contains dsRNA structures, thus our results could be explained by TLR3 sensing these events during viral entry; and initiate signaling leading to IFN, and RIG-I and MDA5 gene expression during the first few hours of infection. Further

experiments are required to prove or disprove this idea however. HBECs were unresponsive to the TLR7/8 ligand R848, strongly suggesting this cell type lacks these TLRs, and that TLR3 rather than TLR7/8 is involved in RIG-I and MDA5 induction. TLR3 has previously been implicated in RV recognition in BEAS-2B cells [56] and HBECs [9]. Interestingly, unlike BEAS-2B cells, we found that TLR3 was not virus inducible in undifferentiated HBECs. In both models however, TLR3 is constitutively expressed, enforcing the hypothesis that TLR3 is an initial sensor of viral nucleic acid in this cell type.

A range of experiments in HBECs demonstrated that RIG-I/MDA5 induction was TLR3/TRIF dependent. Very recently, co-operation between RIG-I/MDA5 and TLR3 has been suggested in a murine model of coxsackievirus infection [57]. TLR3 was absolutely required for defense against coxsackievirus infection, by inducing IFN-γ. The authors suggest that TLR3 mediated induction by IFN-γ may work in parallel with RIG-I/MDA5 inducing type I IFN, and further suggested that these responses may be coupled, although potential mechanisms for this were not explored. We believe however that our study is the first to provide definitive evidence of endosomal and intracellular PRRs working in concert. We argue that as RV enters via endosomes, yet most of the dsRNA load occurs in the cytoplasm, the idea of two related pattern recognition systems seem plausible. RV replicates in the cytoplasm, and produces multiple centers of RNA dependent RNA replication, therefore increases in the RNA helicases can be viewed as a mechanism to continually monitor the intracellular RNA load (likely dsRNA and ssRNA), and through RNA helicases, induce IFN and cytokines consistently, during the course of infection. The upregulation of IFN-β, IFN-λ and T cell and neutrophil cytokines are highly important for the control of virus replication and acute inflammatory responses within the airway (for a summary, see Figure S4). It would be extremely interesting to study other common human respiratory viruses which preferentially infect bronchial epithelial cells, or viruses that infect other mucosal surfaces such as the gut, to investigate if maximal IFN and cytokine responses require both TLR3, and RIG-I/MDA5.

Finally, we assessed the role of IFN-α/β signaling in RIG-I and MDA5 induction. RIG-I and MDA5 are ISGs, a consistent observation in many different cell types and models [24,57–60]. We have also observed that in HBECs, RIG-I and MDA5 are IFN-β and IFN-λ inducible (data not shown). As RIG-I and MDA5 are IFN inducible, our in vitro experiments could not rule out the possibility of the effects of low level IFN inducing RIG-I and MDA5. Our data *in vivo*, however clearly show that RIG-I and MDA5 can be induced in the absence of IFN-β and IFN-λ, *IFNAR1*$^{-/-}$ mice, which cannot respond to type I IFN and are unable to produce IFN-λ in the lung, still produced RIG-I and MDA5 mRNA and protein upon RV1B infection. Also, in HBECs with intact IFN responses, RIG-I/MDA5 mRNA was upregulated early, by 4–8 h, and we argue this quick response is likely IFN independent.

We believe this is the first report of sequential involvement or collaboration of TLR and RNA helicase mediated pathways for innate defense against a virus infection. Our overall model is depicted in Figure S4. The model argues that RIG-I and MDA5 that are not well expressed in uninfected cells are both virus inducible via the constitutively expressed TLR3/TRIF, and later IFN inducible. Upon RV infection, TLR3 signaling in the endosome gives quick induction of new RIG-I and MDA5. Importantly, the model highlights the need for RNA helicase induction to be quick, in a few hours in infected cells. After several hours, as virus moves out of the endosome and into the cytoplasm, newly synthesized virus RNA is sensed by RIG-I/MDA5. This is where the majority of viral nucleic acid will be for the rest of the infection cycle, and is likely key in the induction of innate immune response to RV infection. At later time points, the actions of IFN-β and IFN-λs may further induce RIG-I and MDA5 in infected and non-infected cells. In non-infected cells, the presence of IFN may "warn" neighboring cells about the presence of viruses, and prepare the epithelium through upregulation of interferon inducible genes including RIG-I and MDA5.

Our initial interest in PRRs important in RV infection and IFN expression came from studies in asthmatic individuals which showed bronchial epithelial cells from asthmatics had very low levels of IFN-β and IFN-λ expression and increased RV replication compared to non-asthmatic controls [17,18]. It is currently believed that IFN-β, or IFN-λs could contribute to the outcome of asthma exacerbations. While these studies implicate the bronchial epithelium as a key producer of IFN-β and IFN-λs in RV infections, it is unclear which IFN is more important in protection. Understanding the regulation of both type I and type III IFNs is therefore a research goal for identifying why asthmatics have deficient innate responses to RV infection. The results of the present study have identified the importance of RIG-I, MDA5 and TLR3 in RV induced IFN, therefore future studies should scrutinize these pathways in asthmatics and non-asthmatics to ascertain if asthmatics have defective signaling leading to decreased IFN production.

In summary we provide evidence that the dsRNA receptor TLR3 acts to induce both RIG-I and MDA5 gene and protein expression in HBECs in a model of RV infection. Both RIG-I and MDA5 were required for maximal IFN and pro-inflammatory cytokine induction, and control of RV replication indicating that they have non-redundant roles in RV infection. The data support a model that in HBECs, TLR3 but not TLR7/8 operate in concert with RIG-I/MDA5, and are together required for innate responses to RV infection. As asthmatic HBECs have reduced RV inducible IFN-β and IFN-λ expression compared to non-asthmatic cells, both the TLR3 and RNA helicase pathways warrant further exploration in order to ascertain why these cells produce reduced IFN expression.

Materials and Methods

Cells and viruses

HBECs from non-asthmatic, non-smoking individuals were obtained from a commercial source (Clonetics, Wokingham, UK), and cultured in BEGM with supplements according to the suppliers recommended protocol (Clonetics). Unless otherwise stated, all data was derived from experiments from 3 different HBEC sources. BEAS-2B cells (European Collection of Cell Cultures) were cultured in RPMI with 10% FCS (Invitrogen, Paisley, UK). HeLa cells were grown in DMEM with 10% FCS (Invitrogen), and used for RV titration assays. Major group RV16 and minor group RV1B were grown in HeLa cells, after three cycles of freeze and thawing, supernatant and cellular material where clarified by centrifugation at 4,000 rpm for 15 min, filter sterilized, aliquoted and frozen at -80°C. The serotype of all RV stocks was confirmed by titration with serotype specific anti-sera (American Type Culture Collection), and all RV stocks and cells were confirmed to be free of *Mycoplasma* contamination using a commercially available detection kit (Roche, Burgess Hill, UK).

Transient transfections with siRNA or plasmid DNA

HBECs were cultured to 80% confluency in 12 well plates and transfected with 100 nM specific siRNA or control siRNA (specific

for luciferase, Dharmacon, Lafayette, CO, USA), for 24 h prior to infection with RV1B. Time courses and dose responses of siRNA were performed previously to determine optimum conditions for knockdown of target genes. All siRNA achieved at least a 75% knockdown of target mRNA, and each siRNA was assessed for the induction of IFN or pro-inflammatory cytokine mRNA in the absence of infection. HBECs were cultured to near confluency in 12 well plates and then transfected with 0.25 μg per well of ΔTRIF-pUNO1 (a constitutive active TRIF cDNA, Invivogen, San Diego CA, USA), or pUNO1 control plasmid (Invivogen) or left untransfected for 5 h. All transfections were with Lipofectamine 2000 (Qiagen, Crawley, UK) according to the manufacturers recommended protocol. Complexes were removed, medium replaced and cells left for 24 h. RNA was then extracted and RIG-I, MDA5 mRNA measured. ΔRIG-I, RIG-IC and pEF-BOS control vector [24] were used to transfect BEAS-2B cells, at 0.25–0.5 μg per well, using Superfect (Qiagen) according to the manufacturer's recommended protocol.

Infection of HBECs and BEAS-2B cells

HBECs were cultured to 80% confluency in 12 well plates, using BEGM (Clonetics) and starved in BEBM (no supplements) overnight and infected with RV1B for 1 h with shaking at room temperature, and samples taken at appropriate time points. Alternatively, HBECs were transfected with siRNA (Dharmacon), placed in BEGM without serum and then infected with RV1B. BEAS-2B cells were placed in 2% FCS containing RPMI medium overnight and infected with RV1B or RV16 for 1 h as above and placed in 2% FCS containing RPMI medium until required. For experiments involving enumerating virus replication, adhered virus was washed off by three additions of medium after the 1 h infection period.

RNA extraction, cDNA synthesis and quantitative PCR

Total RNA was extracted from HBECs (RNeasy kit, Qiagen), and 2 μg was used for cDNA synthesis (Omniscript RT kit, Qiagen). Total RNA was also extracted from the upper left lobe of the mouse lung, and placed in RNA later (Qiagen), prior to RNA extraction and cDNA synthesis (as above). Quantitative PCR was carried out using specific primers and probes for each gene (Table S4 in Supporting Information S1). Reactions consisted of 12.5 μl of 2X Quanti-Tect Probe PCR Master Mix (Qiagen) in 25 μL. cDNA for 18S amplifications were diluted 1/100 in sterile water. Reactions were analyzed using an ABI 7000 TaqMan, (ABI Foster City, CA, USA) at 50°C for 2 min, 94°C for 10 min, and 45 cycles of 94°C for 15 s and 60°C for 15 s. Each gene was normalized to 18S rRNA, and for HBEC studies, presented as copies of each mRNA per 2×10^5 cells, and for mouse lung, per cDNA reaction using a standard curve based on amplification with plasmid DNA. For siRNA experiments, copy number was expressed as a % of copy number versus control siRNA.

SDS PAGE, Western blotting and immunofluorescence

For western blotting, total protein lysates were run on 4–12% Bis-Tris polyacrylamide gels, and transferred onto nitrocellulose membranes (Invitrogen), blocked in 5% skim milk, and probed with antibodies specific for mouse and human RIG-I (Cell Signaling, Danvers, MA, USA), diluted to 0.083 μg/mL, MDA5 1 μg/mL (Santa Cruz Biotechnology Inc, CA, USA), α-tubulin 0.2 μg/mL (Santa Cruz Biotechnology Inc), or β-actin, 1 μg/mL (Biovision, Mountain View CA, USA). Secondary antibodies used were goat anti-mouse HRP, 0.08 μg/mL, sheep anti-rabbit HRP, 2 μg/mL (AbD Serotec, Oxford, UK) and swine anti-goat HRP 1.4 μg/mL (Invitrogen). Blots were developed using ECL (GE Healthcare, Chalfont St Giles, UK). For immunohistochemistry, HBECs were grown on 8 well chamber slides (Nunc, Rochester NY, USA), infected with RV or treated with 10 ng/mL IFN-β, 5 μg/mL polyIC or medium for 8 or 24 h, and washed with PBS, fixed in 4% paraformaldehyde at room temperature for 5–7 min, washed once with PBS, and permeabilized with 0.2% Triton X-100 for 5 min at room temperature, and washed again in PBS. Slides were then blocked with a 1% BSA, 10% FCS-PBS overnight at 4°C. Cells were then stained with either anti-RIG-I, 2 μg/mL (Santa Cruz Biotechnology, Inc) or anti-MDA5, 2.7 μg/mL (Santa Cruz Biotechnology Inc) for 1 h at room temperature. Slides were washed three times with PBS, and stained with for 1 h at room temperature with donkey anti-goat Alexa Fluor 488, 6.7 μg/mL, and washed as above. Slides were then mounted with 4,6-diamidino-2-phenyindole dilactate containing mounting medium, and analysed using a colour CCD camera microscope (Zeiss, Rugby, UK).

Analysis of human bronchial epithelium from individuals challenged with RV16 *in vivo*

Paraffin embedded bronchial biopsies were obtained from 15 non-asthmatic non-smoking individuals used in a previous *in vivo* challenge study with RV16 [16]. Samples were coded, and analyzed blind according to infection status, for RIG-I and MDA5 prior to infection (baseline) or at day 4 after infection. Goat antibodies to RIG-1 and MDA5 (Santa Cruz Biotechnology, Inc) at 2 μg/mL and 1 μg/mL were used respectively. Swine anti-goat LSAM-HRP reagents (DakoCytomation, Ely, UK), were used as per the manufacturer's recommended protocol, and antibody binding visualized using perioxidase staining. Staining intensity on surface epithelium was scored accordingly as 0–3, with no staining scored as 0 and intense staining scored as 3.

Infection of *IFNAR1* deficient and wildtype mice with RV1B

Female *IFNAR1*$^{-/-}$ and 129/SvJ control mice aged 6–9 weeks were inoculated intranasally with 5×10^6 $TCID_{50}$ of RV1B, essentially as previously described [39], and culled humanely by lethal injection at various time points.

Ethics statement

The human experimental challenge study was approved by St Mary's NHS Trust. All volunteers gave informed, written consent. All animal work was in accordance with Project License PPL70/6387, and performed according to regulations outlined by the Home Office, UK, in agreement with the Animals (Scientific Procedures) Act 1986.

Statistical analysis

All *in vitro* experiments were performed 5–6 times, Figures 1, 3–7 used 3 independent HBEC donors, and data generated in the supporting information file also utilized 3 independent HBEC donors. For siRNA experiments, data from each independent experiment was converted to a % of the control siRNA + RV data, and mean ± SEM generated. All other data were expressed as mean ± SEM. Experiments using siRNA or transfection with plasmids were analyzed by one ANOVA and Bonferroni's multiple comparison test, and time course data using two-way ANOVA and Bonferroni's multiple comparison test, using GraphPad Prism software with $p<0.05$ taken as significant. For differences between two groups, a student's t-test was employed with $p<0.05$ taken as significant. Experiments in the mouse model involved 3–4 animals per group, in two independent experiments,

(total of 6–8 animals) data were analyzed using two-way ANOVA and Bonferroni's multiple comparison test in GraphPad Prism. Staining of human bronchial epithelium for RIG-I and MDA5 was analyzed by using the paired Mann-Whitney U test, $p<0.05$ taken as significant.

Supporting Information

Supporting Information S1 Tables S1 to S4.
Found at: doi:10.1371/journal.ppat.1001178.s001 (0.09 MB DOC)

Figure S1 Role of TRIF and Cardif in RV1B induced IFN gene expression in HBECs. (A) siRNA specific to TRIF and Cardif reduced RV1B induced IFN-β compared to control siRNA at 24h post infection. (B) siRNA specific to TRIF and Cardif reduced RV1B induced IFN-λ1 compared to control siRNA at 24h post infection. (C) siRNA specific to TRIF reduced RV1B induced IFN-λ2/3 compared to control siRNA however siRNA specific to Cardiff did not significantly reduce RV1B induced IFN-λ2/3 at 24h post infection. $*p<0.05$, $***p<0.001$ versus control siRNA + RV1B, NS = not significant versus control siRNA+RV1B, n = 5 independent experiments, from 3 different HBEC donors, 2 experiments per donors 1,2 and one experiment for donor 3.
Found at: doi:10.1371/journal.ppat.1001178.s002 (10.10 MB TIF)

Figure S2 Role of TRIF and Cardif in RV1B induced pro-inflammatory cytokine gene expression in HBECs. (A) siRNA specific to TRIF and Cardif reduced RV1B induced rantes compared to control siRNA at 24h post infection. (B) siRNA specific to TRIF and Cardif reduced RV1B induced IP-10 compared to control siRNA at 24h post infection. (C) siRNA specific to TRIF and Cardif reduced RV1B induced IL-8 compared to control siRNA at 24h post infection. (D) siRNA specific to TRIF and Cardif reduced RV1B induced ENA-78 compared to control siRNA at 24h post infection. $***p<0.001$ versus control siRNA+RV1B, NS = not significant versus control siRNA + RV1B, n = 5 independent experiments, from 3 different HBEC donors, 2 experiments per donors 1,2 and one experiment per donor 3.
Found at: doi:10.1371/journal.ppat.1001178.s003 (0.23 MB TIF)

Figure S3 RIG-I mediates the anti-viral responses in RV infection in BEAS-2B cells. (A). Constitutively active RIG-I, (ΔRIG-I) suppressed RV16 vRNA compared to pEF-BOS control at 24h post infection. (B). ΔRIG-I suppressed RV16 release compared to pEF-BOS control at 48h post infection. (C). ΔRIG-I suppressed RV1B vRNA compared to pEF-BOS control at 24h post infection. (D). ΔRIG-I suppressed RV16 release compared to pEF-BOS control at 48h post infection. $*p<0.05$, $**p<0.01$, $***p<0.001$ as indicated n = 4-6 independent experiments.
Found at: doi:10.1371/journal.ppat.1001178.s004 (0.21 MB TIF)

Figure S4 Proposed model of sequential involvement of TLR3/TRIF and RIG-I/MDA5 in RV infecton. TLR3 and TRIF initially are involved in RV signalling in the recognition of RV infection and signal transduction within the endosome, and induce IFN-β, IFN-λ and RIG-I and MDA5 early with the infection cycle (4-12h). After 12h, increases in RIG-I and MDA5 protein in the intracellular compartment recognise a concominant increase in intracellular RV dsRNA and ssRNA. This process induces robust IFN-β and IFN-λ and possibly further RIG-I and MDA5 gene expression.
Found at: doi:10.1371/journal.ppat.1001178.s005 (6.49 MB TIF)

Author Contributions

Conceived and designed the experiments: LS NWB JZ SDM RPW AS MGB TF PKJ SLJ MRE. Performed the experiments: LS NWB JJH JZ SDM RPW AS SD DLC MRE. Analyzed the data: LS NWB JJH RPW SD MRE. Contributed reagents/materials/analysis tools: DLC MGB OMK TF PKJ. Wrote the paper: LS SLJ MRE.

References

1. Rakes GP, Arruda E, Ingram JM, Hoover GE, Zambrano JC, et al. (1999) Rhinovirus and respiratory syncytial virus in wheezing children requiring emergency care. IgE and eosinophil analyses. Am J Respir Crit Care Med 159: 785–790.
2. Seemungal TA, Harper-Owen R, Bhowmik A, Jeffries DJ, Wedzicha JA (2000) Detection of rhinovirus in induced sputum at exacerbation of chronic obstructive pulmonary disease. Eur Respir J 16: 677–683.
3. Gern JE, Galagan DM, Jarjour NN, Dick EC, Busse WW (1997) Detection of rhinovirus RNA in lower airway cells during experimentally induced infection. Am J Respir Crit Care Med 155: 1159–1161.
4. Johnston SL, Pattemore PK, Sanderson G, Smith S, Lampe F, et al. (1995) Community study of role of viral infections in exacerbations of asthma in 9-11 year old children. Bmj 310: 1225–1229.
5. Johnston NW, Johnston SL, Duncan JM, Greene JM, Kebadze T, et al. (2005) The September epidemic of asthma exacerbations in children: a search for etiology. J Allergy Clin Immunol 115: 132–138.
6. Lau SK, Yip CC, Tsoi HW, Lee RA, So LY, et al. (2007) Clinical features and complete genome characterization of a distinct human rhinovirus (HRV) genetic cluster, probably representing a previously undetected HRV species, HRV-C, associated with acute respiratory illness in children. J Clin Microbiol 45: 3655–3664.
7. Griego SD, Weston CB, Adams JL, Tal-Singer R, Dillon SB (2000) Role of p38 mitogen-activated protein kinase in rhinovirus-induced cytokine production by bronchial epithelial cells. J Immunol 165: 5211–5220.
8. Zhu Z, Tang W, Ray A, Wu Y, Einarsson O, et al. (1996) Rhinovirus stimulation of interleukin-6 in vivo and in vitro. Evidence for nuclear factor kappa B-dependent transcriptional activation. J Clin Invest 97: 421–430.
9. Kato A, Favoreto S, Jr., Avila PC, Schleimer RP (2007) TLR3- and Th2 cytokine-dependent production of thymic stromal lymphopoietin in human airway epithelial cells. J Immunol 179: 1080–1087.
10. Zhu Z, Tang W, Gwaltney JM, Jr., Wu Y, Elias JA (1997) Rhinovirus stimulation of interleukin-8 in vivo and in vitro: role of NF-kappaB. Am J Physiol 273: L814–824.
11. Spurrell JC, Wiehler S, Zaheer RS, Sanders SP, Proud D (2005) Human Airway Epithelial Cells Produce Ip-10 (Cxcl10) in Vitro and in Vivo Upon Rhinovirus Infection. Am J Physiol Lung Cell Mol Physiol 289: 85–95.
12. Khaitov MR, Laza-Stanca V, Edwards MR, Walton RP, Rohde G, et al. (2009) Respiratory virus induction of alpha-, beta- and lambda-interferons in bronchial epithelial cells and peripheral blood mononuclear cells. Allergy 64: 375–386.
13. Pizzichini MM, Pizzichini E, Efthimiadis A, Chauhan AJ, Johnston SL, et al. (1998) Asthma and natural colds. Inflammatory indices in induced sputum: a feasibility study. Am J Respir Crit Care Med 158: 1178–1184.
14. Wark PA, Johnston SL, Moric I, Simpson JL, Hensley MJ, et al. (2002) Neutrophil degranulation and cell lysis is associated with clinical severity in virus-induced asthma. Eur Respir J 19: 68–75.
15. Gern JE, Vrtis R, Grindle KA, Swenson C, Busse WW (2000) Relationship of upper and lower airway cytokines to outcome of experimental rhinovirus infection. Am J Respir Crit Care Med 162: 2226–2231.
16. Message SD, Laza-Stanca V, Mallia P, Parker HL, Zhu J, et al. (2008) Rhinovirus-induced lower respiratory illness is increased in asthma and related to virus load and Th1/2 cytokine and IL-10 production. Proc Natl Acad Sci U S A 105: 13562–13567.
17. Wark PA, Johnston SL, Bucchieri F, Powell R, Puddicombe S, et al. (2005) Asthmatic bronchial epithelial cells have a deficient innate immune response to infection with rhinovirus. J Exp Med 201: 937–947.
18. Contoli M, Message SD, Laza-Stanca V, Edwards MR, Wark PA, et al. (2006) Role of deficient type III interferon-lambda production in asthma exacerbations. Nat Med 12: 1023–1026.
19. Corne JM, Marshall C, Smith S, Schreiber J, Sanderson G, et al. (2002) Frequency, severity, and duration of rhinovirus infections in asthmatic and non-asthmatic individuals: a longitudinal cohort study. Lancet 359: 831–834.
20. de Bouteiller O, Merck E, Hasan UA, Hubac S, Benguigui B, et al. (2005) Recognition of double-stranded RNA by human toll-like receptor 3 and downstream receptor signaling requires multimerization and an acidic pH. J Biol Chem 280: 38133–38145.

21. Alexopoulou L, Holt AC, Medzhitov R, Flavell RA (2001) Recognition of double-stranded RNA and activation of NF-kappaB by Toll-like receptor 3. Nature 413: 732–738.
22. Diebold SS, Kaisho T, Hemmi H, Akira S, Reis e Sousa C (2004) Innate antiviral responses by means of TLR7-mediated recognition of single-stranded RNA. Science 303: 1529–1531.
23. Heil F, Hemmi H, Hochrein H, Ampenberger F, Kirschning C, et al. (2004) Species-specific recognition of single-stranded RNA via toll-like receptor 7 and 8. Science 303: 1526–1529.
24. Yoneyama M, Kikuchi M, Natsukawa T, Shinobu N, Imaizumi T, et al. (2004) The RNA helicase RIG-I has an essential function in double-stranded RNA-induced innate antiviral responses. Nat Immunol 5: 730–737.
25. Gitlin L, Barchet W, Gilfillan S, Cella M, Beutler B, et al. (2006) Essential role of mda-5 in type I IFN responses to polyriboinosinic:polyribocytidylic acid and encephalomyocarditis picornavirus. Proc Natl Acad Sci U S A 103: 8459–8464.
26. Yoneyama M, Kikuchi M, Matsumoto K, Imaizumi T, Miyagishi M, et al. (2005) Shared and Unique Functions of the DExD/H-Box Helicases RIG-I, MDA5, and LGP2 in Antiviral Innate Immunity. J Immunol 175: 2851–2858.
27. Rothenfusser S, Goutagny N, DiPerna G, Gong M, Monks BG, et al. (2005) The RNA helicase Lgp2 inhibits TLR-independent sensing of viral replication by retinoic acid-inducible gene-I. J Immunol 175: 5260–5268.
28. Meylan E, Curran J, Hofmann K, Moradpour D, Binder M, et al. (2005) Cardif is an adaptor protein in the RIG-I antiviral pathway and is targeted by hepatitis C virus. Nature 437: 1167–1172.
29. Kawai T, Takahashi K, Sato S, Coban C, Kumar H, et al. (2005) IPS-1, an adaptor triggering RIG-I- and Mda5-mediated type I interferon induction. Nat Immunol 6: 981–988.
30. Xu LG, Wang YY, Han KJ, Li LY, Zhai Z, et al. (2005) VISA Is an Adapter Protein Required for Virus-Triggered IFN-beta Signaling. Mol Cell 19: 727–740.
31. Seth RB, Sun L, Ea CK, Chen ZJ (2005) Identification and Characterization of MAVS, a Mitochondrial Antiviral Signaling Protein that Activates NF-kappaB and IRF3. Cell 122: 669–682.
32. Kato H, Takeuchi O, Mikamo-Satoh E, Hirai R, Kawai T, et al. (2008) Length-dependent recognition of double-stranded ribonucleic acids by retinoic acid-inducible gene-I and melanoma differentiation-associated gene 5. J Exp Med 205: 1601–1610.
33. Hornung V, Ellegast J, Kim S, Brzozka K, Jung A, et al. (2006) 5′-Triphosphate RNA is the ligand for RIG-I. Science 314: 994–997.
34. Pichlmair A, Schulz O, Tan CP, Naslund TI, Liljestrom P, et al. (2006) RIG-I-mediated antiviral responses to single-stranded RNA bearing 5′-phosphates. Science 314: 997–1001.
35. Kato H, Takeuchi O, Sato S, Yoneyama M, Yamamoto M, et al. (2006) Differential roles of MDA5 and RIG-I helicases in the recognition of RNA viruses. Nature 441: 101–105.
36. Kato H, Sato S, Yoneyama M, Yamamoto M, Uematsu S, et al. (2005) Cell type-specific involvement of RIG-I in antiviral response. Immunity 23: 19–28.
37. Sadik CD, Bachmann M, Pfeilschifter J, Muhl H (2009) Activation of interferon regulatory factor-3 via toll-like receptor 3 and immunomodulatory functions detected in A549 lung epithelial cells exposed to misplaced U1-snRNA. Nucleic Acids Res.
38. Morris GE, Parker LC, Ward JR, Jones EC, Whyte MK, et al. (2006) Cooperative molecular and cellular networks regulate Toll-like receptor-dependent inflammatory responses. Faseb J 20: 2153–2155.
39. Bartlett NW, Walton RP, Edwards MR, Aniscenko J, Caramori G, et al. (2008) Mouse models of rhinovirus-induced disease and exacerbation of allergic airway inflammation. Nat Med 14: 199–204.
40. Ank N, Iversen MB, Bartholdy C, Staeheli P, Hartmann R, et al. (2008) An important role for type III interferon (IFN-lambda/IL-28) in TLR-induced antiviral activity. J Immunol 180: 2474–2485.
41. Kumar H, Koyama S, Ishii KJ, Kawai T, Akira S (2008) Cutting edge: cooperation of IPS-1- and TRIF-dependent pathways in poly IC-enhanced antibody production and cytotoxic T cell responses. J Immunol 180: 683–687.
42. Kalali BN, Kollisch G, Mages J, Muller T, Bauer S, et al. (2008) Double-stranded RNA induces an antiviral defense status in epidermal keratinocytes through TLR3-, PKR-, and MDA5/RIG-I-mediated differential signaling. J Immunol 181: 2694–2704.
43. Wornle M, Sauter M, Kastenmuller K, Ribeiro A, Roeder M, et al. (2009) Novel role of toll-like receptor 3, RIG-I and MDA5 in poly (I:C) RNA-induced mesothelial inflammation. Mol Cell Biochem 322: 193–206.
44. Le Goffic R, Pothlichet J, Vitour D, Fujita T, Meurs E, et al. (2007) Cutting Edge: Influenza A virus activates TLR3-dependent inflammatory and RIG-I-dependent antiviral responses in human lung epithelial cells. J Immunol 178: 3368–3372.
45. Liu P, Jamaluddin M, Li K, Garofalo RP, Casola A, et al. (2007) Retinoic acid-inducible gene I mediates early antiviral response and Toll-like receptor 3 expression in respiratory syncytial virus-infected airway epithelial cells. J Virol 81: 1401–1411.
46. Wang Q, Nagarkar DR, Bowman ER, Schneider D, Gosangi B, et al. (2009) Role of double-stranded RNA pattern recognition receptors in rhinovirus-induced airway epithelial cell responses. J Immunol 183: 6989–6997.
47. Onoguchi K, Yoneyama M, Takemura A, Akira S, Taniguchi T, et al. (2007) Viral infections activate types I and III interferon genes through a common mechanism. J Biol Chem 282: 7576–7581.
48. Zhang B, Li M, Chen L, Yang K, Shan Y, et al. (2009) The TAK1-JNK cascade is required for IRF3 function in the innate immune response. Cell Res 19: 412–428.
49. Marques JT, Devosse T, Wang D, Zamanian-Daryoush M, Serbinowski P, et al. (2006) A structural basis for discriminating between self and nonself double-stranded RNAs in mammalian cells. Nat Biotechnol 24: 559–565.
50. Jackson AL, Linsley PS (2010) Recognizing and avoiding siRNA off-target effects for target identification and therapeutic application. Nat Rev Drug Discov 9: 57–67.
51. Prchla E, Kuechler E, Blaas D, Fuchs R (1994) Uncoating of human rhinovirus serotype 2 from late endosomes. J Virol 68: 3713–3723.
52. Suzuki T, Yamaya M, Sekizawa K, Hosoda M, Yamada N, et al. (2001) Bafilomycin A(1) inhibits rhinovirus infection in human airway epithelium: effects on endosome and ICAM-1. Am J Physiol Lung Cell Mol Physiol 280: L1115–1127.
53. Rohll JB, Percy N, Ley R, Evans DJ, Almond JW, et al. (1994) The 5′-untranslated regions of picornavirus RNAs contain independent functional domains essential for RNA replication and translation. J Virol 68: 4384–4391.
54. Palmenberg AC, Spiro D, Kuzmickas R, Wang S, Djikeng A, et al. (2009) Sequencing and analyses of all known human rhinovirus genomes reveal structure and evolution. Science 324: 55–59.
55. Kienberger F, Zhu R, Moser R, Blaas D, Hinterdorfer P (2004) Monitoring RNA release from human rhinovirus by dynamic force microscopy. J Virol 78: 3203–3209.
56. Hewson CA, Jardine A, Edwards MR, Laza-Stanca V, Johnston SL (2005) Toll-like receptor 3 is induced by and mediates antiviral activity against rhinovirus infection of human bronchial epithelial cells. J Virol 79: 12273–12279.
57. Negishi H, Osawa T, Ogami K, Ouyang X, Sakaguchi S, et al. (2008) A critical link between Toll-like receptor 3 and type II interferon signaling pathways in antiviral innate immunity. Proc Natl Acad Sci U S A 105: 20446–20451.
58. Imaizumi T, Kumagai M, Taima K, Fujita T, Yoshida H, et al. (2005) Involvement of retinoic acid-inducible gene-I in the IFN-{gamma}/STAT1 signalling pathway in BEAS-2B cells. Eur Respir J 25: 1077–1083.
59. Kang DC, Gopalkrishnan RV, Lin L, Randolph A, Valerie K, et al. (2004) Expression analysis and genomic characterization of human melanoma differentiation associated gene-5, mda-5: a novel type I interferon-responsive apoptosis-inducing gene. Oncogene 23: 1789–1800.
60. Kang DC, Gopalkrishnan RV, Wu Q, Jankowsky E, Pyle AM, et al. (2002) mda-5: An interferon-inducible putative RNA helicase with double-stranded RNA-dependent ATPase activity and melanoma growth-suppressive properties. Proc Natl Acad Sci U S A 99: 637–642.

Virus-Infection or 5′ppp-RNA Activates Antiviral Signal through Redistribution of IPS-1 Mediated by MFN1

Kazuhide Onoguchi[1,2,3], Koji Onomoto[1], Shiori Takamatsu[1,2], Michihiko Jogi[1,2], Azumi Takemura[1], Shiho Morimoto[1], Ilkka Julkunen[4], Hideo Namiki[3], Mitsutoshi Yoneyama[5,6], Takashi Fujita[1,2]*

1 Department of Molecular Genetics, Institute for Virus Research, Kyoto University, Kyoto, Japan, **2** Graduate School of Biostudies, Kyoto University, Yoshida-Konoe Sakyo, Kyoto, Japan, **3** Graduate School of Science and Engineering, Waseda University, Tokyo, Japan, **4** Department of Vaccination and Immune Protection, National Institute for Health and Welfare, Helsinki, Finland, **5** Division of Molecular Immunology, Medical Mycology Research Center, Chiba University, Chuo-ku, Chiba, Japan, **6** PRESTO, Japan Science and Technology Agency, Saitama, Japan

Abstract

In virus-infected cells, RIG-I-like receptor (RLR) recognizes cytoplasmic viral RNA and triggers innate immune responses including production of type I and III interferon (IFN) and the subsequent expression of IFN-inducible genes. Interferon-β promoter stimulator 1 (IPS-1, also known as MAVS, VISA and Cardif) is a downstream molecule of RLR and is expressed on the outer membrane of mitochondria. While it is known that the location of IPS-1 is essential to its function, its underlying mechanism is unknown. Our aim in this study was to delineate the function of mitochondria so as to identify more precisely its role in innate immunity. In doing so we discovered that viral infection as well as transfection with 5′ppp-RNA resulted in the redistribution of IPS-1 to form speckle-like aggregates in cells. We further found that Mitofusin 1 (MFN1), a key regulator of mitochondrial fusion and a protein associated with IPS-1 on the outer membrane of mitochondria, positively regulates RLR-mediated innate antiviral responses. Conversely, specific knockdown of MFN1 abrogates both the virus-induced redistribution of IPS-1 and IFN production. Our study suggests that mitochondria participate in the segregation of IPS-1 through their fusion processes.

Citation: Onoguchi K, Onomoto K, Takamatsu S, Jogi M, Takemura A, et al. (2010) Virus-Infection or 5′ppp-RNA Activates Antiviral Signal through Redistribution of IPS-1 Mediated by MFN1. PLoS Pathog 6(7): e1001012. doi:10.1371/journal.ppat.1001012

Editor: C. Cheng Kao, Indiana University, United States of America

Received February 17, 2010; **Accepted** June 18, 2010; **Published** July 22, 2010

Funding: The Ministry of Education, Culture, Sports, Science and Technology of Japan (http://www.mext.go.jp/english/), the Ministry of Health, Labour and Welfare of Japan (http://www.mhlw.go.jp/english/index.html), the PRESTO Japan Science and Technology Agency (http://www.jst.go.jp/kisoken/presto/index_e.html), the Uehara Memorial Foundation (http://www.ueharazaidan.com/), the Mochida Memorial Foundation for Medical and Pharmaceutical Research (http://www.mochida.co.jp/zaidan/l), and Nippon Boehringer Ingelheim (http://www.boehringer-ingelheim.co.jp/com/Home/index.jsp). The funders had no role in study design, data collection and analysis, decision to publish, or preparation of the manuscript.

Competing Interests: The authors have declared that no competing interests exist.

* E-mail: tfujita@virus.kyoto-u.ac.jp

Introduction

Type I and III interferons (IFNs) play central roles in innate immune responses to viral infections [1,2,3,4]. In a variety of tissues, IFN production is triggered by a cytoplasmic sensor, retinoic acid inducible gene I (RIG-I)-like Receptor (RLR), which specifically senses viral RNA and induces antiviral signaling [5,6]. Once RLR is activated, its signal is relayed through physical interaction to IFN-β promoter stimulator 1 (IPS-1, also known as MAVS, VISA or Cardif) [7,8,9,10]. IPS-1 interacts with multiple signal transducers and protein kinases that activate transcription factors to induce IFN and other cytokine genes [11]. IPS-1 is expressed on the mitochondrial outer membrane and this localization is essential for signaling to occur [9]. However the reason for this underlying mechanism is unknown. Here, we investigated the cellular distribution of IPS-1 in virus-infected cells. We observed that IPS-1 is usually distributed evenly in all mitochondria in uninfected cells, however upon viral infection or the introduction of 5′ppp-RNA, which mimics viral RNA [12,13,14], a redistribution of IPS-1 occurred, resulting in a speckle-like pattern on mitochondria. Furthermore, we demonstrated that a mitochondrial GTPase, Mitofusin 1 (MFN1), which regulates mitochondrial fission and fusion [15], plays a critical role in the redistribution of IPS-1, as well as in virus-induced IFN production. Our study highlights the novel mitochondrial regulatory function of specifically sorting IPS-1 and providing a signaling platform for antiviral responses.

Results

Dynamic redistribution of IPS-1 in virus-infected or 5′ppp-RNA-transfected cells

To examine the localization of IPS-1 during viral infections, we generated HeLa cell lines stably expressing FLAG-tagged IPS-1 (IPS-1-HeLa clones, Fig. 1). Although the temporary expression of wild type (wt) IPS-1 results in constitutive signaling [7,8,9,10], the stable cell lines did not exhibit the constitutive activation of downstream target genes. However, upon infection with the Sendai virus (SeV), the cells exhibited increased expression of IFN and chemokine genes (*IFNB1*, *IL29*, *IL28A*, *IL28B* and *CXCL11*) and interferon-stimulated genes (*DDX58*, *IFIH1*, *DHX58*, *IFIT1-3*, and *OASL*) (Fig. 1B and C). Furthermore, the IPS-1-HeLa clones exhibited diminished susceptibility to Encephalomyocarditis virus (EMCV) replication (1 to 2 log) (Fig. 1D). The low basal activity and elevated signaling after SeV-infection suggest that FLAG-IPS-1 is under a regulatory control similar to that of endogenous IPS-1.

Author Summary

Virus-infections, such as influenza and chronic hepatitis C, are prominent diseases and outbreaks of newly emerging viruses are serious problems for modern society. Higher animals, including humans, are genetically equipped with mechanisms, collectively known as innate immunity, to counteract viral infections. RIG-I-like receptor (RLR), a cytoplasmic sensor, contributes to immune regulation by detecting infections by RNA viruses and triggering a series of responses which results in the activation of innate antiviral genes. Furthermore, it has been demonstrated that IPS-1, the adaptor protein of RLR, is expressed on mitochondrial outer membrane. Mitochondrion is an organelle of prokaryotic cell origin; it regulates energy production, and is involved in cell growth and cell death. Why IPS-1 is located on the mitochondrial outer membrane and how mitochondria are involved in antiviral signaling are yet to be explained clearly. In this report, we discovered that mitochondrial fusion protein MFN1 plays a novel function to mediate IPS-1 redistribution, which appears to be a critical step in RLR signaling.

Like endogenous IPS-1, FLAG-tagged IPS-1 is expressed on mitochondria in uninfected cells as shown by co-staining with MitoTracker (Fig. 2A, Mock). However, compared to the even cytoplasmic staining in the mock-infected cells, the staining pattern of IPS-1 became noticeably speckled in SeV-infected cells (Fig. 2A, SeV). Quantification of the fluorescence image revealed that mitochondria heavily stained with MitoTracker but lightly stained with anti-FLAG antibody were produced in SeV-infected cells. This redistribution was also observed with another mitochondrial marker, endoplasmic reticulum-associated amyloid β-peptide-binding protein (ERAB) (Fig. 2B), and different viruses (Newcastle disease virus (NDV), Sindbis virus, EMCV, Influenza virus, and Vesicular stomatitis virus (VSV)) (Fig. 3).

We also examined the distribution of IPS-1 in 5′ppp-RNA-transfected cells. Unlike synthetic single stranded RNA (5′OH-RNA), 5′ppp-RNA is a chemical ligand for RIG-I and is known to mimic viral signaling [12,13,14]. Interestingly, as with a viral infection, 5′ppp-RNA induced a redistribution of IPS-1, suggesting that the redistribution was triggered through RIG-I signaling. It is worth noting that EMCV, which selectively activates another RLR, melanoma differentiation-associated gene 5 (MDA5), also caused the redistribution of IPS-1, suggesting that this effect is common to RLRs. We suspected that IPS-1-HeLa cells exhibit enhanced redistribution of IPS-1 due to enhanced signaling (>10 IFN-β mRNA accumulation, Fig. 1B). This led us to analyze the distribution pattern of endogenous IPS-1 in HeLa cells, and we observed that the distribution pattern of endogenous IPS-1 changed in SeV-infected cells, although exclusive staining by mitochondrial marker was not observed (Fig. 4A). Similar to IPS-1-HeLa cells, we observed that hepatocellular carcinoma SKHep1 cells NDV, SeV, Influenza virus, or Sindbis virus infection also induced a speckled staining pattern in endogenous IPS-1 (Fig. 4B), and displayed enhanced IRF-3 dimerization when compared with HeLa cells (our unpublished data). This suggests that the redistribution is not simply an artifact due to the overexpression of FLAG-IPS-1.

Localization of viral nucleocapsid, RIG-I, and IPS-1

In order to activate RLR signaling, we used NDV to infect cells because it is available an anti-nucleocapsid protein (NP) antibody, a probe for the viral RNA-NP complex. NDV infection resulted in foci of NP in the cytoplasm and induced foci of RIG-I to form (Fig. 5A) [16]. RIG-I was evenly distributed in the cytoplasm, however some of the foci co-localized with those of NP (Fig. 5A). A similar formation of foci and co-localization with viral nucleoprotein complex was observed with other viruses (Ko.O. unpublished observations). IPS-1 accumulated on the periphery of the foci of RIG-I (Fig. 5B) and NP (Fig. 5C). We speculate that activated RIG-I recruits IPS-1, because RIG-I and IPS-1 interacted with each other through CARD-CARD interaction [7,8]. IPS-1 did not co-localize with RIG-I nor NP presumably because mitochondria do not penetrate these foci nor is IPS-1 released from mitochondria. Immunoelectron microscopy using the anti-NP antibody clearly identified the NP foci (Fig. 6A), and anti-FLAG staining (Fig. 6B) showed that mitochondrial IPS-1 accumulated on the periphery of NP foci in NDV infected cells.

A dominant negative mutant of RIG-I does not induce IPS-1 redistribution

To determine if the observed redistribution of IPS-1 is functionally relevant, we used a point mutant of RIG-I (K270A), which normally recognizes ligand RNA but functions as a dominant negative inhibitor (Fig. 7A) [14]. It was observed that NDV infection induced foci of both wt and K270A RIG-I to form (Fig. 7B), however wt but not K270A promoted the speckled staining pattern of IPS-1 (Fig. 7C). The results indicate that the redistribution of IPS-1 is strongly correlated with the activation of antiviral signaling.

Mitofusin 1, but not Mitofusin 2, plays a critical role in RIG-I-induced antiviral signaling

RIG-I was originally identified by screening an expression cDNA library [17]. In addition to the cDNA encoding RIG-I, there were several other candidate cDNA clones which enhance virus-responsive reporter activity. Two of the independent clones encoded a full-length protein, Mitofusin 1 (MFN1). Human MFN1 is composed of 741 amino acids and domains of GTPase and transmembranes (Fig. 8A). MFN1 together with its related protein Mitofusin 2 (MFN2) is expressed on the outer membrane of mitochondria and regulates mitochondrial dynamics [18,19]. Hyper- and hypo-functioning of either MFN1 or MFN2 result in elongated/aggregated and fragmented mitochondria, respectively. GTPase activity was previously shown to be essential for mitochondrial morphological change, particularly the fragmentation of mitochondria induced by a GTP-binding-deficient mutant of MFN1 (MFN1 T109A) [18].

Consistent with the screening results, overexpression of MFN1, but not MFN2, augmented IFN-β promoter activity (Fig. 8B). The GTPase activity is involved in this MFN1 function, since MFN1 T109A significantly inhibited the signaling induced by NDV or 5′ppp-RNA (Fig. 8C and D). It is worth noting that overexpression of MFN1, which results in elongated mitochondria, is not by itself sufficient to deliver the signal. To confirm that the increased signaling observed by MFN1 overexpression was correlated with RIG-I activation, we transfected cells with a combination of RIG-I and MFN1. The RIG-I/MFN1 combination showed enhanced IFN-β promoter activity, but the RIG-I K270A mutant/MFN1 combination failed to do so (Fig. 8E). MEFs derived from mice with disrupted *Mfn1* or *Mfn2* gene was used to confirm the specific involvement of MFN1 in virus-induced antiviral signaling (Fig. 9A and B). The results indicated that MFN1, but not MFN2, is essential for the signal transduction mediated by RIG-I.

We examined other regulatory proteins for mitochondrial fission/fusion mechanism. Optic atrophy protein 1 (OPA1) is

A

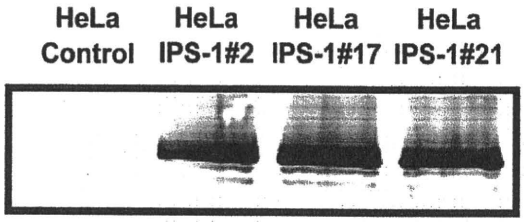

B

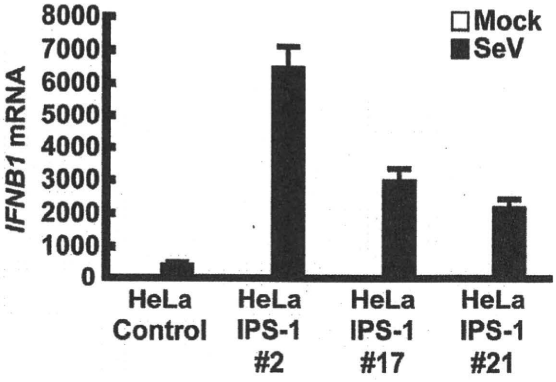

C

	HeLa Control		HeLa IPS-1#2		HeLa IPS-1#17	
	Mock	SeV	Mock	SeV	Mock	SeV
IL29	1.0	3.6	0.8	18.2	0.7	7.2
IL28A	1.0	2.0	0.7	11.7	0.6	6.9
IL28B	1.0	3.4	0.8	23.9	0.7	12.8
DDX58	1.0	1.1	0.7	1.8	0.7	3.8
IFIH1	1.0	2.3	0.8	5.1	1.8	8.8
DHX58	1.0	1.5	0.7	2.4	0.7	3.1
IFIT1	1.0	21.3	1.1	51.0	7.4	65.1
IFIT2	1.0	11.7	1.0	27.0	1.5	32.3
IFIT3	1.0	9.2	0.9	29.8	2.8	43.3
OASL	1.0	5.9	1.2	20.5	2.3	29.9
CXCL11	1.0	2.7	0.7	10.6	1.2	15.9

>9.0
6.0~8.9
3.0~5.9
1.4~2.9
0.7~1.3
<0.6

D

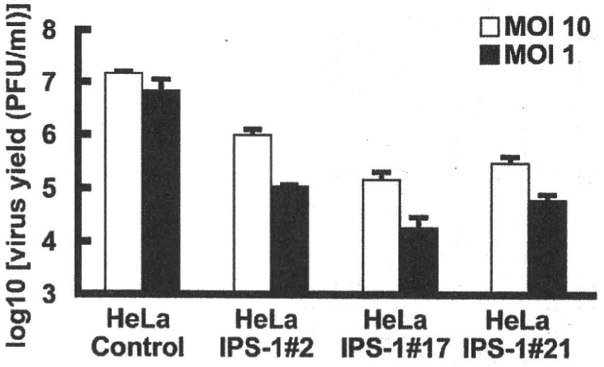

Figure 1. Stable HeLa cell clones expressing FLAG tagged IPS-1. A, Expression of FLAG-IPS-1 was examined in control and IPS-1-expressing HeLa clones (#2, 17, and 21) by immunoblotting using anti-FLAG antibody. **B**, Expression of *IFNB1* in control and IPS-1-HeLa cells was examined by quantitative real time PCR (qRT-PCR). Open and filled bars indicate mock-treated and SeV-infected cells for 12 h, respectively. Data represent means ± s.d. (n = 3). **C**, Expression profiles of cytokine and chemokine genes in control and IPS-1-HeLa cells. Total RNA extracted from indicated cells mock-treated or SeV-infected for 12 h was subjected to analysis using a DNA microarray. Relative mRNA levels using a control expression of 1.0 are shown. **D**, Replication of EMCV in control and IPS-1-HeLa clones. The indicated cell clones were infected with EMCV at a MOI of 1 or 10. The viral titer in the culture medium at 24 h post-infection was determined with the plaque assay. Data represent means ± s.d. (n = 3).
doi:10.1371/journal.ppat.1001012.g001

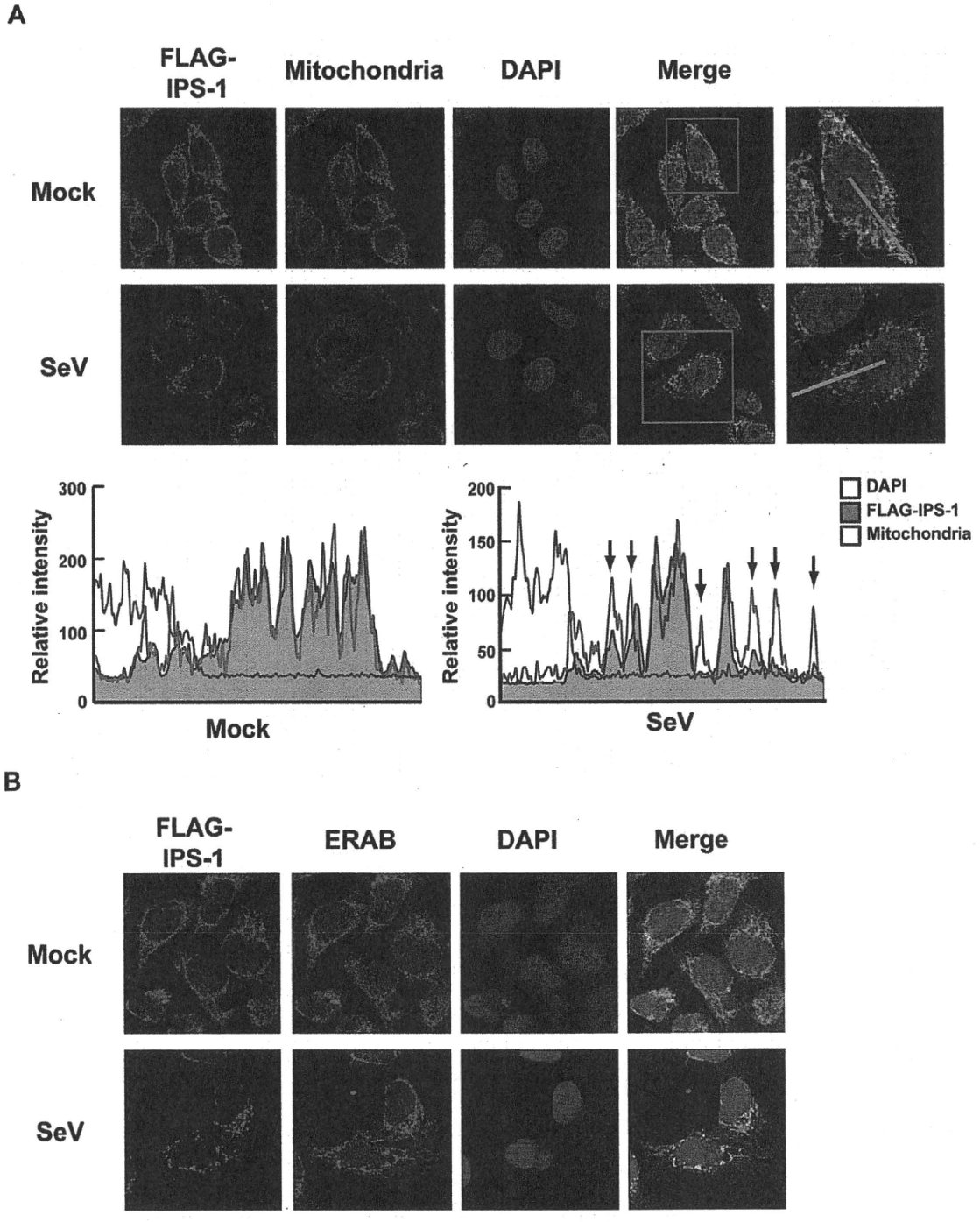

Figure 2. Redistribution of IPS-1 in SeV-infected cells. A, The IPS-1-HeLa clone #2 was mock-treated or infected with SeV for 12 h and stained with MitoTracker (Mitochondria) and anti-FLAG antibody (FLAG-IPS-1). Nuclei were visualized by staining with DAPI throughout this study. The fluorescent image was quantified in the area indicated by blue line (right most panel). Quantification results from mock- or SeV-infected cells are shown at the bottom. Fluorescence of DAPI corresponds to area in the nucleus. The mitochondria heavily stained with MitoTracker but lightly stained with anti-FLAG are shown by arrows. **B,** IPS-1-HeLa cells were mock-treated or infected with SeV for 12 h. Cells were stained with anti-FLAG antibody (FLAG-IPS-1) and anti-ERAB antibody (ERAB).
doi:10.1371/journal.ppat.1001012.g002

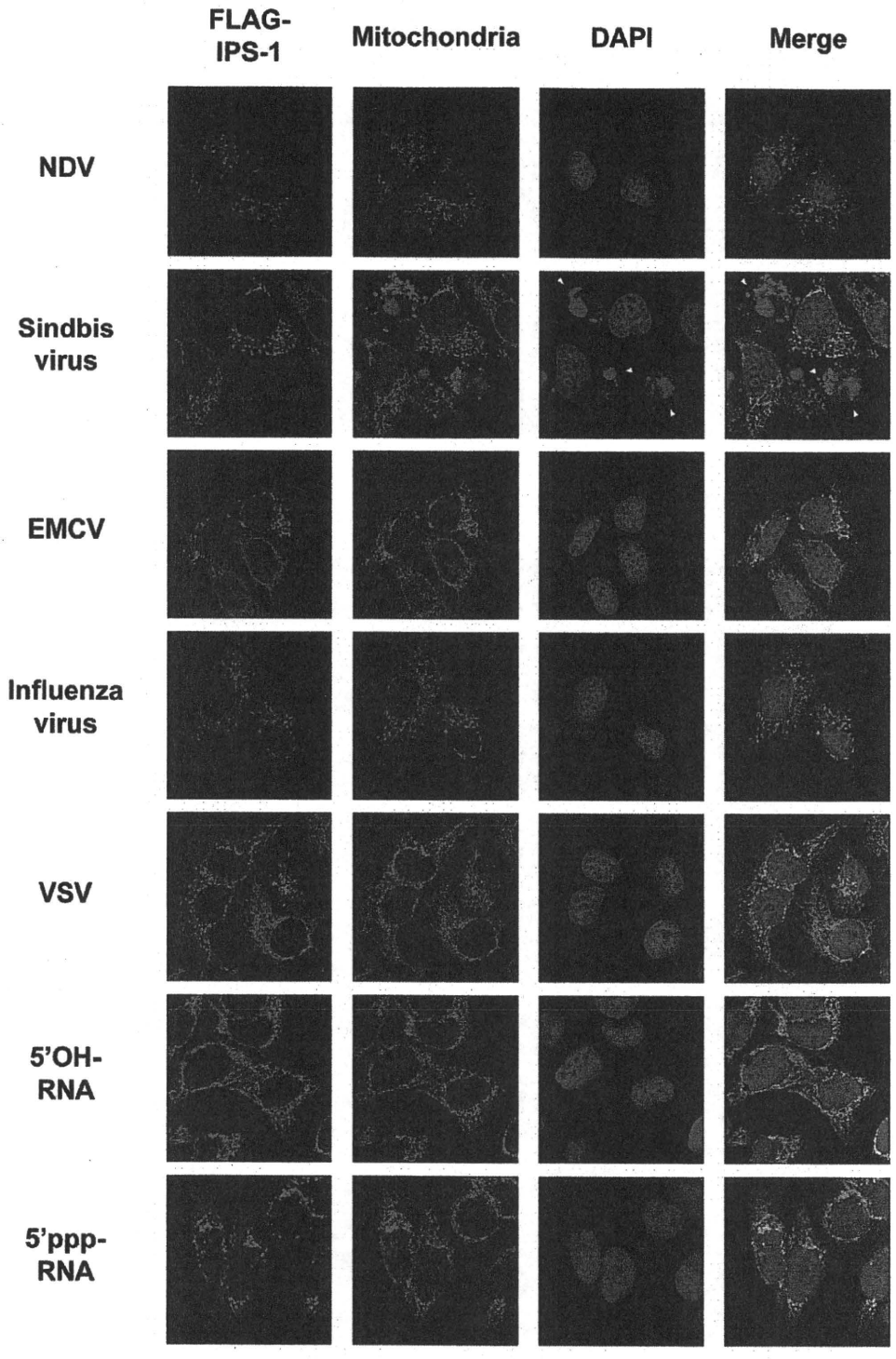

Figure 3. Redistribution of IPS-1 induced by virus-infection and 5'ppp-RNA-transfection. IPS-1-HeLa cells were infected with the indicated viruses or transfected with 5'OH-RNA or 5'ppp-RNA chemically synthesized by in vitro transcription using T7 RNA polymerase. At 12 h post-infection or -transfection, the cells were stained with anti-FLAG antibody and MitoTracker (Mitochondria). Arrowheads show dead cells with shrunk nuclei in Sindbis virus-infected cells.
doi:10.1371/journal.ppat.1001012.g003

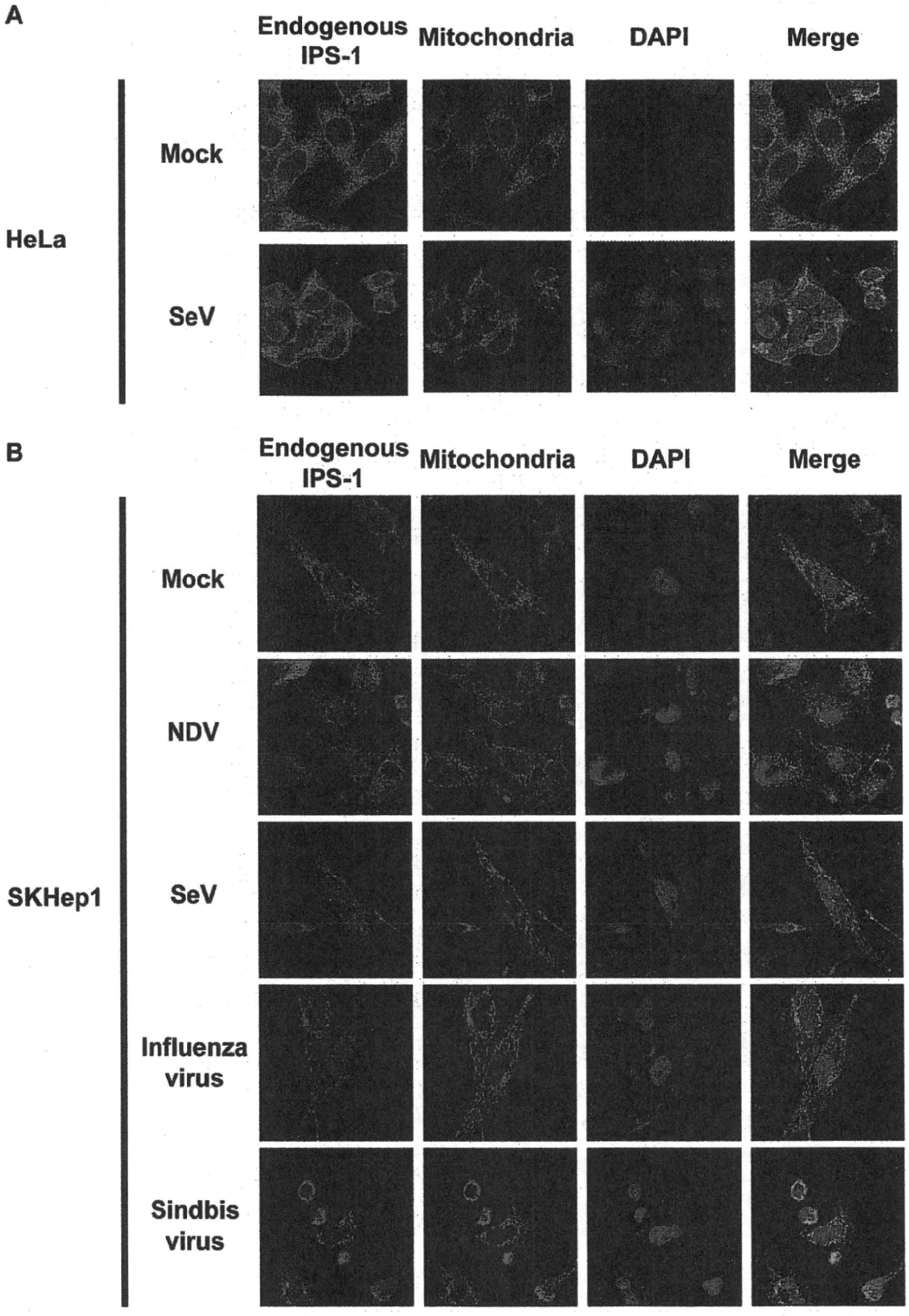

Figure 4. Redistribution of endogenous IPS-1 in virus-infected cells. A, HeLa cells were infected with Mock or SeV for 12 h. The cells were stained with anti-IPS-1 antibody and MitoTracker (Mitochondria). **B**, SKHep1 cells were infected with NDV, SeV, Influenza virus, or Sindbis virus for 12 h. The cells were stained with anti-IPS-1 antibody and MitoTracker (Mitochondria).
doi:10.1371/journal.ppat.1001012.g004

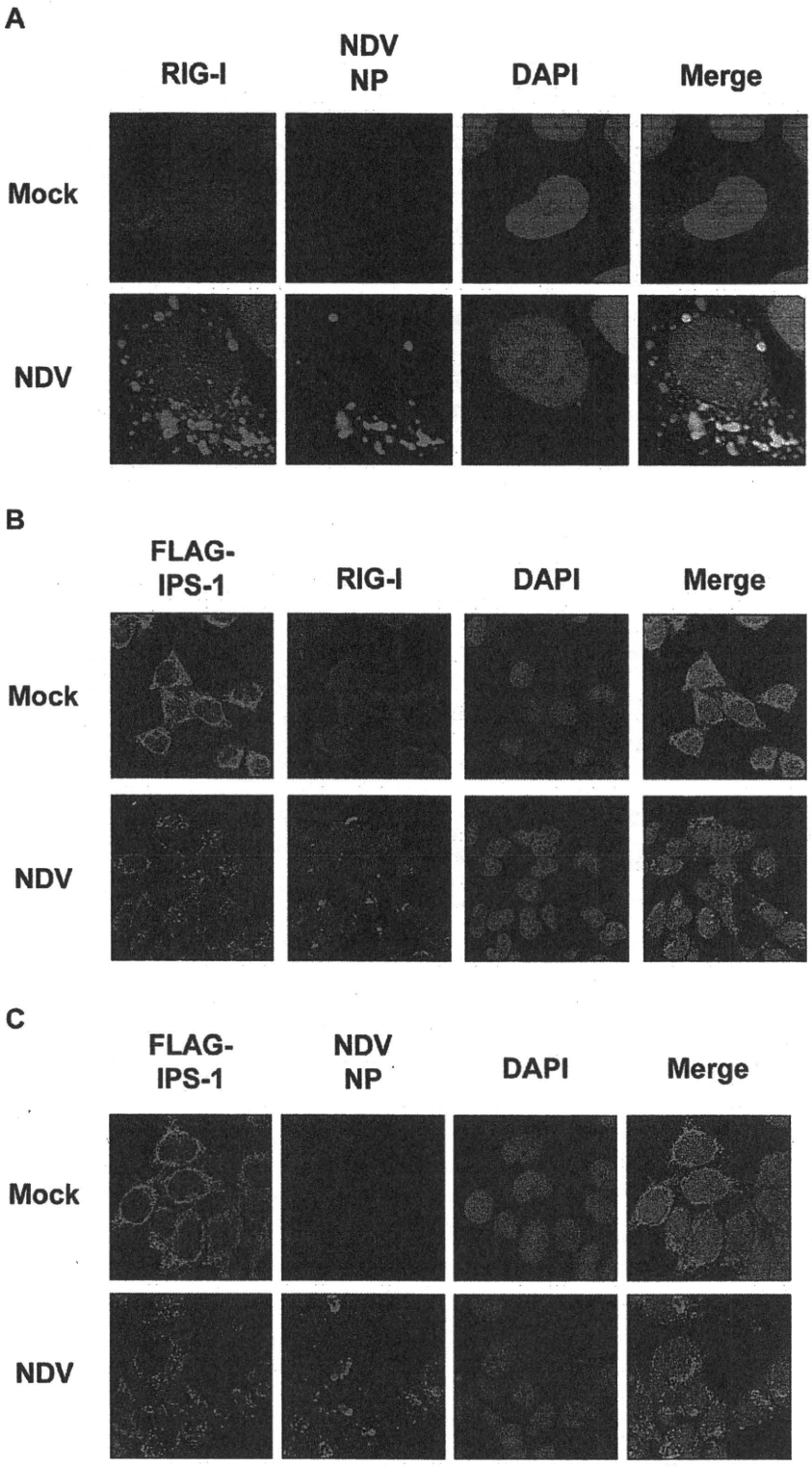

Figure 5. Localization of viral nucleocapsid, RIG-I, and IPS-1. A, HeLa cells were infected with NDV for 12 h and stained with anti-RIG-I antibody (RIG-I) and anti-NP antibody (NDV NP). **B** and **C**, IPS-1-HeLa cells were infected with NDV for 12 h and stained with anti-FLAG antibody and anti-RIG-I antibody or anti-NP antibody.
doi:10.1371/journal.ppat.1001012.g005

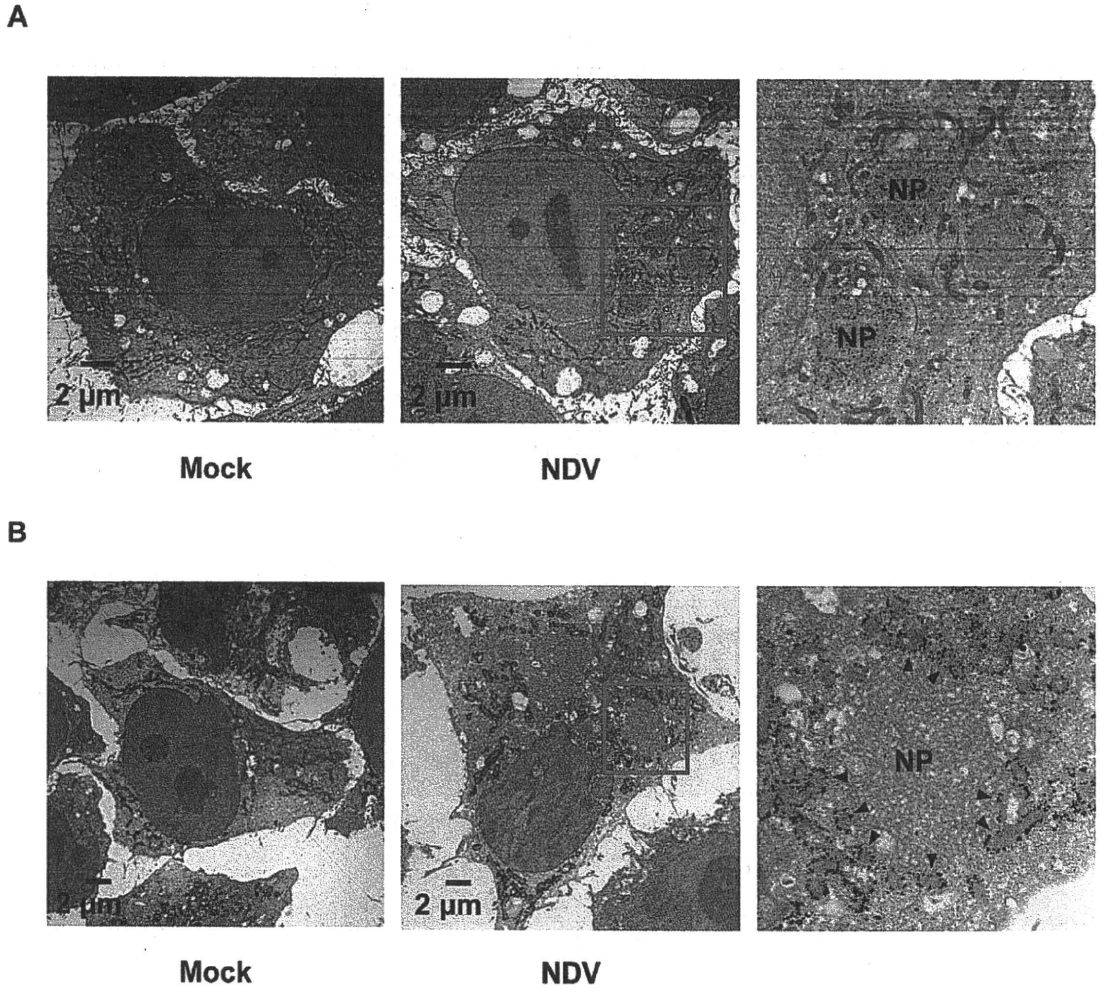

Figure 6. Localization of IPS-1 and mitochondria. A, IPS-1-HeLa cells infected with NDV for 9 h were fixed, stained with anti-NP antibody, and subjected to ultrathin sectioning as shown in the Methods. The area enclosed by a red rectangle is enlarged. NP: NP foci stained with the anti-NP antibody were visualized using gold particles. **B,** IPS-1-HeLa cells infected with NDV for 9 h were fixed, stained with anti-FLAG antibody, and subjected to ultra thin sectioning. The area enclosed by a red rectangle is enlarged. NP: morphologically similar structures are in **A**. IPS-1 was visualized using gold particles. The arrowheads indicate boundaries between IPS-1 and NP foci.
doi:10.1371/journal.ppat.1001012.g006

expressed on, and implicated in the fusion of the mitochondrial inner membrane [20]. Three independent siRNA targeting OPA1, down-regulated OPA1 expression (Fig. 9C) and partially (up to 50%) blocked NDV-induced signaling (Fig. 9D). However, the knockdown of dynamin-related protein 1 (DRP1) (Fig. 9E), which regulates mitochondrial fission [21] resulting in elongated mitochondria, did not have a significant effect (Fig. 9F). To explore the site where MFN1 is active, we temporarily overexpressed the dominant active RIG-I (RIG-I CARD) [17] or IPS-1 in wt and Mfn-knockout MEFs. Unlike the signal generated by the overexpression of IPS-1, the signal generated by overexpression of the RIG-I tandem caspase recruitment domain (CARD) clearly required MFN1. MFN1 however, is dispensable if IPS-1 is overexpressed (Fig. 9G). Again, MFN2 exhibited little influence on the signaling triggered by either stimulus. These results indicate that MFN1, but not MFN2, is essential for signal transduction mediated by RIG-I and IPS-1.

Physical interaction between IPS-1 and MFN1

To explore the molecular mechanism of how IPS-1 is regulated by MFN1, co-immunoprecipitation was performed using cells stably expressing IPS-1. FLAG-IPS-1 was precipitated by anti-FLAG and the associated proteins were analyzed by immunoblotting (Fig. 10). Both MFN1 and MFN2 constitutively associated with IPS-1 in the cells, but an unrelated mitochondrial outer membrane protein, BCL-XL, did not associate with IPS-1. Furthermore, OPA1 and DRP1 did not co-immunoprecipitate with FLAG-IPS-1. These data suggest that IPS-1 selectively associates with MFN1 and MFN2.

Knockdown of MFN1 inhibits the redistribution of IPS-1 induced by viral infection

Next, we examined what effect the knockdown of MFN1 would have on the virus-induced redistribution of IPS-1. Three independent siRNA efficiently knocked down MFN1 expression

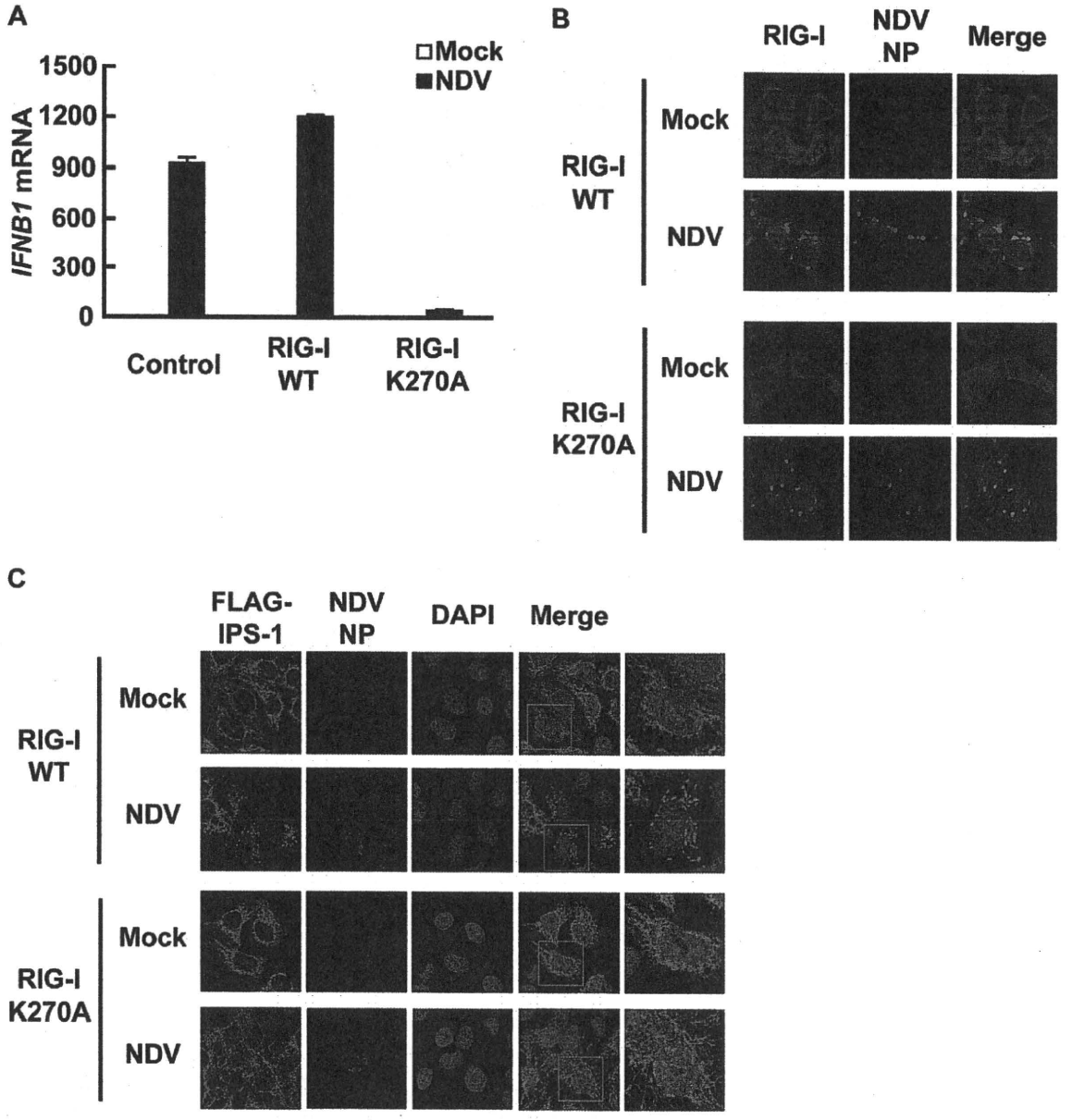

Figure 7. A dominant negative mutant of RIG-I fails to induce IPS-1 redistribution. A, IPS-1-HeLa cells stably expressing wild-type human RIG-I (RIG-I WT) or mutant RIG-I (RIG-I K270A) were mock-treated or infected with NDV for 12 h and expression of *IFNB1* mRNA was analyzed by qRT-PCR. Open and filled bars indicate RNA samples from mock-treated and NDV-infected cells, respectively. Data represent means ± s.d. (n = 3). **B**, IPS-1-HeLa cells expressing RIG-I WT or RIG-I K270A were infected with NDV for 12 h and stained with anti-RIG-I antibody and anti-NP antibody. RIG-I staining is diffuse in uninfected cells however infection by NDV produced RIG-I foci. Some RIG-I foci are co-localized with NDV NP foci. **C**, IPS-1-HeLa cells expressing RIG-I WT or RIG-I K270A were infected with NDV for 12 h and IPS-1 redistribution was examined. IPS-1 and NP were stained with anti-IPS-1 antibody and anti-NP antibody, respectively. The area enclosed by the red rectangle is enlarged at the right. Although the redistributed IPS-1 surrounds NP foci in RIG-I WT cells, K270A mutation of RIG-I failed to induce the redistribution of IPS-1, but not the formation of NP foci.
doi:10.1371/journal.ppat.1001012.g007

(Fig. 11A) resulting in a strong inhibition of the NDV-induced IFN-β gene expression in HeLa cells and IPS-1-HeLa cells (Fig. 11B and 11C). This once again suggests that IPS-1-HeLa cells tend to behave like normal cells. Upon NDV infection, IPS-I displayed a speckled staining pattern in control cells, but not in the MFN1-knockdown cells (Fig. 11D). Though the intensity of NP staining did not increase, MFN1-knockdown significantly inhibited IFN gene activation. This correlates with prior observations that although IFN production is inhibited by LGP2 overexpression, viral yield does not increase [22]. When control siRNA-treated cells were infected with NDV, a redistribution of IPS-1 was observed (69.3±15.7% of cells positive for NP). In MFN1-knockdown cells, although NDV infection resulted in the formation of NP foci, IPS-1 redistribution did not occur

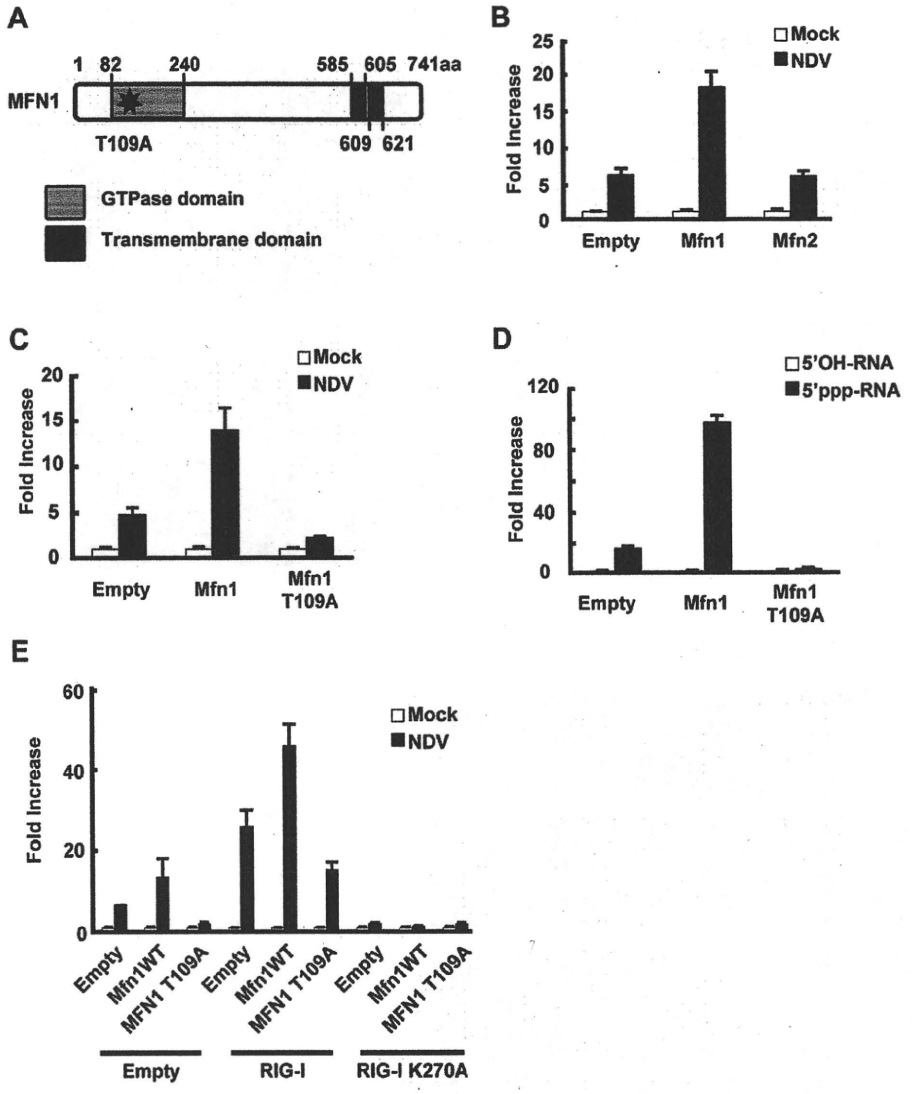

Figure 8. MFN1 is involved in antiviral signaling. A, Schematic representation of the MFN1 domain. **B**, L929 cells were transfected with a virus-responsive reporter gene (p-125 Luc) and either an empty vector (Empty), an expression vector for MFN1, or an expression vector for MFN2 as indicated. 48 h after the transfection, cells were mock-treated or infected with NDV. Luciferase activity was determined at 12 h after infection. **C** and **D**, L929 cells were transfected with a virus-responsive reporter gene (p-125 Luc) and either an empty vector (Empty) or an expression vector for MFN1 or its mutant (MFN1 T109A) as indicated. At 48 h after transfection, cells were mock-treated, infected with NDV, or transfected with 5'OH-RNA or 5'ppp-RNA. Luciferase activity was determined at 12 h (**C**) or 9 h (**D**) after induction. **E**, L929 cells were transfected with a virus-responsive reporter gene (p-125 Luc) and combinations of the indicated vectors. 48 h after the transfection, cells were mock-treated or infected with NDV. Luciferase activity was determined 12 h after infection.
doi:10.1371/journal.ppat.1001012.g008

(4.5±1.3% of cells positive for NP). A similar effect was observed when MFN1-knockdown cells were infected with SeV (Fig. 12). These results strongly suggest that MFN1 is critical to the redistribution of IPS-1 triggered by RIG-I mediated sensing of viral RNA.

Discussion

RIG-I mediated antiviral signaling is a critical antiviral response which is initiated when the RIG-I sensor recognizes viral RNA. A signal is relayed to IPS-1, a mitochondrial regulator which delivers the signal downstream. Interestingly, the IPS-1-HeLa clones in this study exhibited very low basal expression of IFN genes, which led us to speculate that IPS-I inhibitory protein(s) is up regulated in these clones. We also examined the expression level of NLRX1, an IPS-1 inhibitor [23], and noted no change in its expression level (not shown). Similarly, levels of MFN1 and MFN2 did not change in the IPS-1-HeLa clones. (Fig. 10, input).

We observed that the IPS-1 level did not change for up to 12 h in virus-infected cells and no specific modification of IPS-1 was identified up to that point. We therefore hypothesize that the activation status of IPS-1 is determined by its localization pattern. We speculate that the mechanism of mitochondrial fusion is mediated by MFN1, and that IPS-1 translocates from some